1. SHAPE MEMORY ALLOYS

Shape memory alloys have the unique ability to undergo large deformation while returning to their original undeformed shape through either the shape memory effect or the superelastic effect. Shape memory alloys are able to undergo these deformations because of the reversible diffusionless detwinning process they undergo when deformed. The shape memory effect is associated with the martensitic form of shape memory alloys and requires the input of heat in order to recover the deformation. Austenitic (superelastic) shape memory alloys are associated with the superelastic effect and require only the removal of the load or stress on the material in order to recover the deformation. This unique recovery behavior along with the hysteretic stress-strain behavior during tensile loading make shape memory alloys an optimal candidate for seismic design and retrofit of structures as a recentering and energy dissipation device. In particular, shape memory alloys provide excellent low- and high-cycle fatigue properties, an elastic strain range up to 8-10% strain, strain hardening at large strain levels, hysteretic damping, and a stress plateau to limit force transfer to other parts of a structure. Currently, the best way of implementing these materials into structures has not been fully explored. One possible solution is to introduce shape memory alloys into the structure as the fibers of a composite material which would allow the typically manufactured smaller diameter SMA wires to be used in applications where larger cross-sections are required while also providing some constraint against buckling and further energy dissipation due to deformation of the matrix material. In order to implement shape memory alloys into composite type materials, a good understanding of the mechanical behavior of the individual SMAs needs to be gained.

Superelastic 0.254 mm (0.01 inch) Diameter NiTi wires

Test Specimens

A number of 0.254 mm (0.01 inch) diameter superelastic NiTi wires were tested in this study in order to determine the cyclic properties of small diameter wires which can be used as fiber reinforcement in polymer matrix composite systems. All specimens were obtained from the same 20 foot length of wire and tested as received from the manufacturer. The wire specimens were straight annealed and had a black oxide surface to prevent corrosion. No additional annealing or processing of the material was applied before performing the study.

Loading Protocol

Since the wires were studied to determine their potential use in composite systems to be implemented in earthquake engineering applications, an adequate loading protocol was chosen to simulate the typical strain levels and strain rates which can be experienced by structural members during an earthquake. A loading protocol representing a far field type ground motion was used which consisted of increasing tensile strain cycles of 0.5%, 1.0%-5% by increments of 1%, six cycles to 6% strain, and four cycles to 7% strain. The first set of tests was run quasi-statically at a loading rate of 0.025 Hz. Dynamic tests were performed to represent the dynamic nature of an earthquake loading and to determine any changes in the mechanical behavior of the NiTi wire specimens at higher loading rates. Dynamic tests were performed at 0.5 Hz, 1.0 Hz, and 2.0 Hz. A typical plot of the loading protocol can be seen in Figure 1.
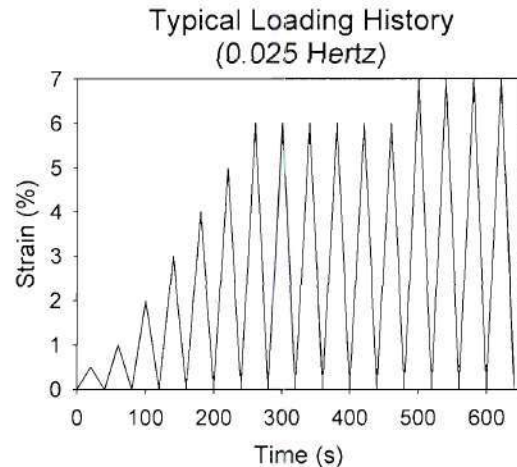
Figure 1: Typical quasi-static loading protocol for cyclic tensile testing of the 0.254 mm (0.01 inch) diameter NiTi wires

Experimental Test Setup

An ELectroForce 3200 table-top testing apparatus, which consisted of an electromagnetic actuator with a stroke capacity of 12.7 mm (0.5 inches), was used to perform the cyclic tensile tests on the small diameter wire specimens. The loading protocol was run in displacement control with strain being measured based on cross-head displacement since the wires were too thin in order to facilitate the use of an extensometer. Wintest software was used in order to apply the loading protocol and acquire the data output at the specified scan rate. A 48.9 N (11 lbf) load cell was used in order to measure the load on the specimen during testing. The ELF 3200 was fitted with DMA grip fixtures for the tensile cyclic test. To facilitate gripping of the specimen, the wire specimens were compressed between two aluminum plates and held in place with two screws and epoxy which can be seen in Figure 2. All specimens had a gage length of approximately 38.1 mm (1.5 inches). Two quasi-static tests were run on previously untested wire specimens. During dynamic testing, previously untested wire specimens were tested at each of the loading rates. After the initial test, the dynamic specimen were retested under the same loading protocol and same loading rate two subsequent times without regripping the specimen in order to see how the stress-strain behavior compared to that of previously uncycled NiTi shape memory alloy wires. With each test, the crossheads were adjusted such that there was no slack and no load on the wire and the displacement was reset to its zero level accordingly.
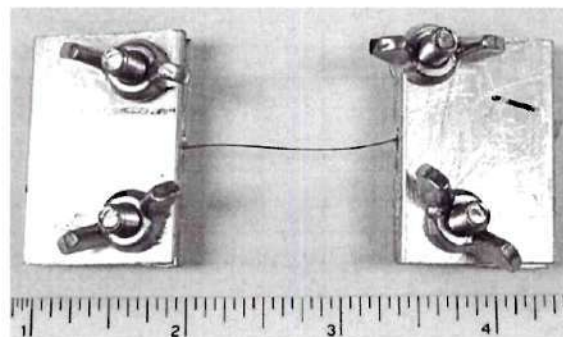

Figure 2: Test specimen for the 0.254 mm (0.01 inch) diameter NiTi shape memory alloys

For this study, the performance of the 0.254 mm (0.01 inch) diameter superelastic NiTi wire undergoing a cyclic tensile loading is evaluated. The mechanical properties that are evaluated include the residual strain (ε_R), the forward and reverse transformation stress (σ_L, and σ_{UL}), the initial elastic modulus (E_i), and the equivalent viscous damping associated with a given cycle (ξ_{eq}). The residual strain refers to the strain at zero stress at the end of a given strain cycle. It will be considered the main measure of the ability of the NiTi SMA to provide recentering capabilities. The forward transformation stress is the stress at which the phase transformation from austenite to detwinned martensite initiates. The unloading plateau is the estimate of the inflection point on the unloading curve representing the start of the reverse transformation from detwinned martensite back to austenite upon unloading. The initial elastic modulus provides a measure of the slope of the initial elastic curve before the loading plateau is reached. Equivalent viscous damping is a common value used in earthquake engineering to measure the energy dissipation provided by a material or structure by normalizing the energy dissipated with respect to the stiffness of the material.

Quasi-static Test Results

Figure 3 provides the stress-strain results for a previously untested 0.254 mm (0.01 inch) diameter superelastic NiTi wire undergoing the cyclic loading protocol previously presented at a loading rate of 0.025 Hz. The plot shows good superelastic properties with a clear loading and unloading stress plateau present. The plot appears to be shifted to the right suggesting possible slack in the wire at the onset of testing or a small amount of initial slipping which may have occurred during the first loading cycle. This suggests that the residual strain values and maximum cyclic strain values may actually be slightly lower than those obtained from an analysis of the plot. Even with this shift, the residual strain remained below 1% even after four 7% strain cycles suggesting good recentering capability of the small wires. The loading plateau stress of the first 6% strain cycle is approximately 531 MPa (77 ksi) with a small degradation in this value with increased loading cycles. This degradation can be associated with the formation of permanent localized slip which tends to assist the forward transformation process. The equivalent viscous damping value reached approximately 4.5% during the 6% strain cycles providing some energy dissipation due to the flag shape hysteresis. Very little change in the initial elastic modulus can be seen with increased cycling. The plot clearly shows degradation in the properties with increased cycling, but does not show typical strain hardening even when cycled out to 7% strain. This suggests that force transfer to other members of the structure even under large strains will be minimized.
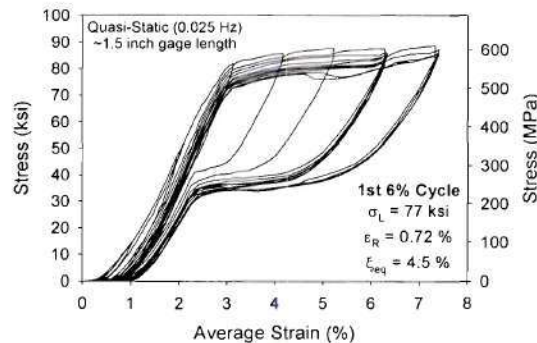

Figure 3: Stress-strain plot for a previously untested NiTi wire tested quasi-statically

Dynamic Test Results

Earthquakes are a dynamic event, and as such, it is important to understand how the mechanical properties of the NiTi wires may change at higher loading rates. The stress-strain plots for three previously untested 0.254 mm (0.01 inch) diameter NiTi wire cycled dynamically at 0.5 Hz, 1.0 Hz, and 2.0 Hz, respectively, can be seen in Figure 4. As with the quasi-static test, all three plots show good superelastic behavior. No real variation in the loading plateau stress was found with the increased strain rates, although the unloading plateau was less defined with increased loading rates. The less defined unloading plateau suggest that self-heating of the wire specimen is occurring at the higher loading rates since the material does not have time to dissipate the heat produced by the exothermic-endothermic phase transformation. Since the phase transformation is a thermoelastic process, the increased temperature tends to affect the formation of the unloading plateau by not allowing a clear plateau to form. The loss of a clear unloading plateau also led to a small decrease in the equivalent viscous damping values with increased cycling due to the loss of hysteretic area. There is also a significant increase in the residual strain with increased strain rates. For the first 6% strain cycle, the residual strain measured for the 0.5 Hz specimen was only 0.49% while for the 2.0 Hz specimen the residual strain was measured to be 1.05%. Although the residual strain increased with the increased loading rate, the maximum residual strain for all dynamically tested specimens remained below 1.4% even when cycled four times at 7% strain. This shows that the NiTi wire specimens maintain good recentering capabilities at strain rates and strain levels equivalent to those that may be experienced during a seismic event.
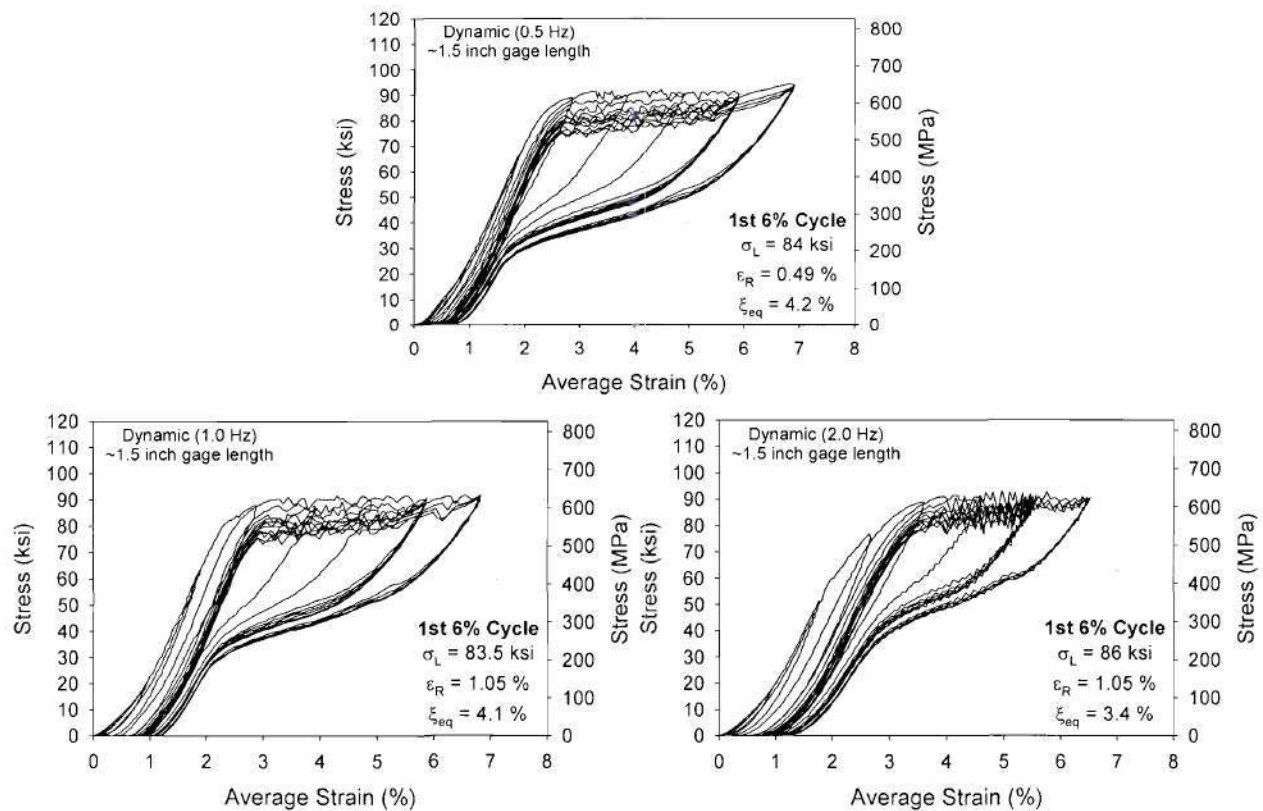

Figure 4: Stress-strain plot for a previously untested NiTi wire tested dynamically at 0.5 Hz, 1.0 Hz, and 2.0 Hz

As was previously mentioned, the dynamic specimens were each retested a second and third time in order to determine if the NiTi wires provided good superelastic properties even after being cycled to as high as 7% strain. Figure 5 shows the stress-strain curves for the first and second retest of the 1.0 Hz specimen. The results show an interesting stabilization of the mechanical properties of the NiTi SMA wire for the retested specimens as compared to the previously untested stress-strain curve shown in Figure 4. The rate at which the residual strain increased tended to decrease during the first and second retests of the wire with the maximum value of the residual strain for the retested specimens being below 0.5% strain for the third test. The loading plateau and unloading plateau stabilized during the first and second retest. In particular, the unloading plateau was more evident for the previously cycled specimens which provide a more consistent damping to the system. The results from the retested specimens suggest that continued cycling of NiTi wires can help stabilize the superelastic properties which would be important for seismic applications of the material. This result further suggests that mechanically training NiTi SMAs may result in a more consistent mechanical behavior.
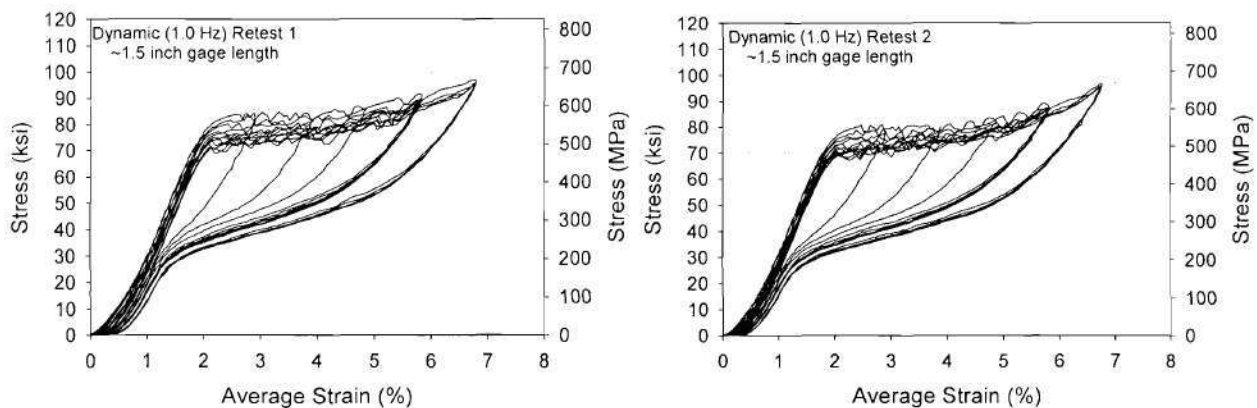

Figure 5: Stress-strain plot for the 1.0 Hz NiTi retested specimen

Cyclic Properties Study

The plots shown in Figure 6 provide the initial elastic modulus, loading plateau stress, residual strain, and equivalent viscous damping values with respect to the maximum cyclic strain for the 0.254 mm (0.01 inch) diameter previously untested NiTi wires tested quasi-statically and dynamically at 0.5 Hz, 1.0 Hz, and 2.0 Hz. As shown in Figure 6(a), the initial elastic modulus increases with increased strain rate. The elastic modulus for the specimen tested quasi-statically ranges between approximately 22.1 GPa (3200 ksi) to 24.8 GPa (3600 ksi) where the results for the 0.5 Hz dynamic test range between approximately 31.0 GPa (4500 ksi) and 33.1 GPa (4800 ksi). The higher loading rates act to initially stiffen the material which would provide a shorter period structure and typically lower initial displacements during an earthquake type loading. All loading rates show a decrease in elastic modulus with an increase in maximum strain level and increased number of cycles mainly due to the formation of permanent dislocations and slip which tends to soften the material.

Figure 6(b) shows the effect that loading rate has on the loading plateau stress with increased maximum strain cycles. The loading plateau stress results show a significant increase in the loading plateau stress with increased strain rate, although there was little difference between the three dynamically tested specimens. The loading plateau stress was measured as the stress at 3% strain for the quasi-static, 0.5 Hz, and 1.0 Hz tests and the stress at 3.5% strain for the 2.0 Hz test based on the stress-strain plots shown in Figure 4 and 5. The loading plateau stress also decreased more for the dynamic loading rates than for the quasi-static loading rate with continued cycling. The drop was approximately 10% for the quasi-static test and approximately 15% for the dynamic 1.0 Hz test from the 3% cycle where the loading plateau stress was first reached to the last 7% cycle. This dynamic effect can be attributed to the thermoelastic nature of the material while the general decrease in the loading plateau stress with continued cycling can be attributed to localized slip assisting the phase transformation from austenite to stress induced martensite.

The variation in residual strain with respect to maximum cyclic strain and loading rate can be seen in Figure 6(c). The plot shows an increase in residual strain with increased cycling as a result of the formation of permanent localized slip mentioned previously. As with past studies, the results present no true sensitivity to loading rate as the 0.5 Hz loading rate test had the lowest value of residual strain for the last 7% strain cycle, 0.68%, where the 1.0 Hz and 2.0 Hz loading rate tests had the highest values of residual strain for the last 7% strain cycle, 1.2% and 1.3%, respectively. The results suggest that at intermediate strain rates the residual strain values may decrease, but as the strain rates increase the residual strain may increase resulting in a degradation of the recentering capability of the wire NiTi SMA specimens at high strain rates. Although the higher strain rates provided larger residual strain values, all residual strain values remained below 1.4% showing good recentering capability for all rates up to 2.0 Hz which would be typical of an earthquake type loading.

Figure 6(d) shows very little difference between the equivalent viscous damping values for the quasi-static test and the dynamic tests. The quasi-static test has a slightly large value of equivalent viscous damping at the higher maximum strain cycles, 5.2% for the first 7% cycle, compared to the 2.0 Hz tested specimen which had an equivalent viscous damping value of 3.6% for the first 7% strain cycle. This reduction in equivalent viscous damping with increased strain rate can be associated with the increase and distortion of the unloading plateau stress and the decrease in the loading plateau stress with increased strain rates resulting in a decrease in the hysteretic area. For all specimens, the equivalent viscous damping values increased with increased maximum strain level as a result of the larger hysteretic area. Although, past studies have shown that when the material reaches its fully stress induced martensitic state that the equivalent viscous damping values decrease with increased maximum strain level due to the onset of strain hardening. It is important to note that the equivalent viscous damping values for the austenitic NiTi wire remains fairly low suggesting that it can not be used solely for damping purpose in earthquake engineering applications.
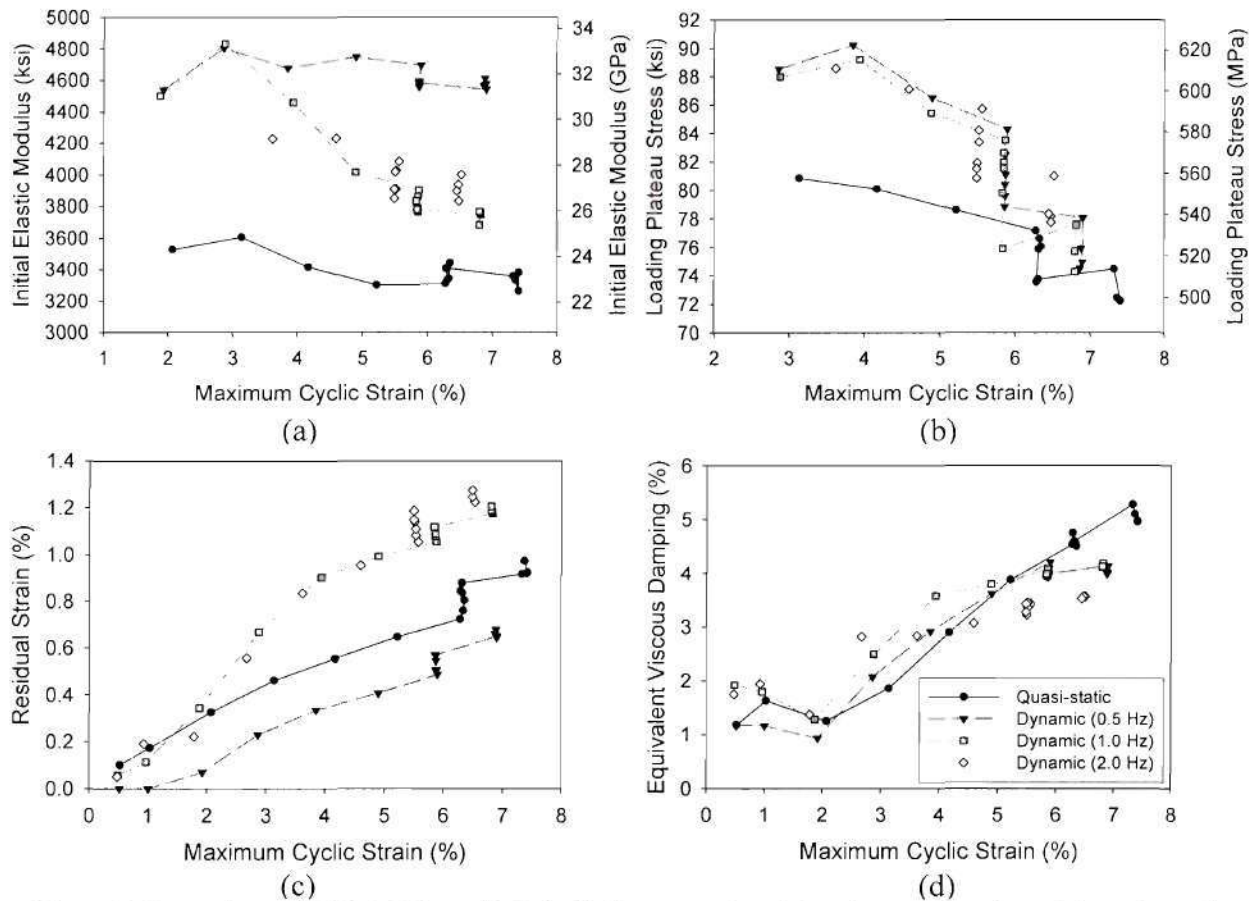
Figure 6: Comparison of NiTi 0.254 mm (0.01 inch) diameter wire subjected to quasi-static and dynamic cyclic loading showing: (a) initial elastic modulus, (b) loading plateau stress, (c) residual strain, and (d) equivalent viscous damping

Superelastic 2.16 mm (0.085 inch) Diameter NiTi wires

Test Specimens

Eight 2.16 mm (0.085 inch) diameter superelastic NiTi wires were tested in this study to determine their cyclic properties with respect to loading rate and maximum strain cycle. These tests were conducted in a similar manner as was presented for the 0.254 mm (0.01 inch) diameter specimens. The larger diameter NiTi specimens are important in obtaining a larger cross-sectional area of shape memory alloy fibers in a polymer matrix composite system. This is particularly important for round specimens which could be implemented as cross-bracing devices or energy dissipation devices in earthquake engineering systems. The eight specimens were all obtained from the same 20 foot length of wire in order to prevent any bias based on composition changes and were tested as received from the manufacturer. No additional annealing or processing was done to these specimens. As with the 0.254 mm (0.01 inch) diameter specimens, these specimens were straight annealed by the manufacturer and had a black oxide surface. The eight 2.16 mm (0.085 inch) diameter NiTi wire specimens were also compared to some previously tested 2.16 mm (0.085 inch) diameter NiTi wire which were annealed at 350°C

(662°F) for 30 minutes and immediately water quenched in order to determine if annealing before testing provides more optimal superelastic properties. All of the 2.16 mm (0.085 inch) diameter NiTi specimens had austenite finish temperatures below room temperature ensuring that they would be superelastic during testing.

Loading Protocol

The same far field type ground motion loading protocol used for the 0.254 mm (0.01 inch) diameter specimens was used to test the 2.16 mm (0.085 inch) diameter specimens with the exception that the last four 7% strain cycles were increased to 8% strain cycles because of the capacity of the testing apparatus. The loading protocol thus consisted of increasing strain cycles of 0.5%, 1.0%-5% by increments of 1%, six cycles to 6% strain, and four cycles to 8% strain as can be seen in Figure 7. The first set of tests was run quasi-statically at a loading rate of 0.025 Hz followed by dynamic tests run at 0.5 Hz, 1.0 Hz. and 2.0 Hz.
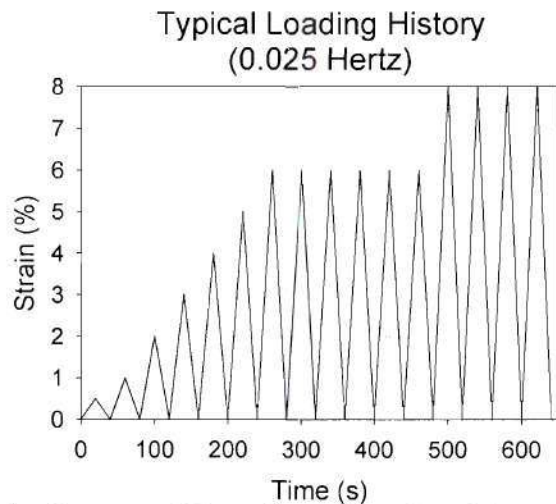

Figure 7: Typical quasi-static loading protocol for cyclic tensile testing of the 2.16 mm (0.085 inch) diameter NiTi wires

Experimental Test Setup

A 250 kN (55 kip) MTS hydraulic testing apparatus fitted with MTS 647 hydraulic wedge grips was used to perform all tests on the 2.16 mm (0.085 inch) diameter NiTi wires. Flat specimen wedges with a surfalloy finish was used to grip the wires specimens with a pressure of 13.8 MPa (2000 psi). As with the 0.254 mm (0.01 inch) diameter specimens, the loading protocol was run in displacement control with strain being measured based on cross-head displacement because attempts to use strain control based on extensometer output showed slipping of the extensometer during loading which could not be resolved. The loading protocol was input using an MTS TestStar controller running *TestWare* software which used output from the cross-head movement to control the actuator. The loads were measured by the internal 250 kN (55 kip) load cell of the testing system. All specimens were cut to lengths of 165.1 mm (6.5 inches) where a 50.8 mm (2 inch) length on both ends of the specimen was used for gripping the specimen leaving a 63.5 mm (2.5 inch) gage length. All tests were performed on previously untested wire specimens with each loading rate test being performed on two separate specimens to ensure the accuracy of the

results. The only difference in the testing of the annealed specimens was that they were tested in strain control with a 25.4 mm (1 inch) gage extensometer used to measure the strain level and provide strain feedback to the MTS controller. The same properties as those used to evaluate the 0.254 mm (0.01 inch) diameter NiTi tests (residual strain, loading plateau stress, initial elastic modulus, and equivalent viscous damping) were used to evaluate the behavior of the 2.16 mm (0.085 inch) diameter NiTi specimens. An explanation of these properties was previously presented.

Quasi-static Test Results

The stress-strain curve for a previously untested 2.16 mm (0.085 inch) diameter NiTi superelastic SMA wire is shown in Figure 8. A clear flag shape hysteresis can be seen due to the formation of both a clear loading and unloading plateau, particularly at the larger strain cycles. Small amounts of strain hardening can be seen upon loading the specimens above 7% strain suggesting that at this point the material has completed the phase transformation from austenite to stress induced martensite. The loading plateau stress for the first 6% strain cycle is approximately 462 MPa (67 ksi) with a considerable degradation of this value to approximately 310 MPa (45 ksi) for the last 8% strain cycle. A clear unloading plateau is apparent, particularly for the 8% strain cycles. The unloading plateau stress also decreased with continued cycling, but not to the extent of which the loading plateau stress did. The equivalent viscous damping measured for the first 6% cycle was 5.2%, suggesting that even the larger diameter wire specimens still do not provide adequate damping capacity to be used solely as an energy dissipation device. Only slight changes in the initial elastic modulus are apparent from the stress-strain curve. The NiTi specimen showed good recentering capability even after four cycles out to 8% strain. The maximum residual strain remained below 1.25% with the residual strain after the first 6% cycle being only 0.82%. This suggests that NiTi SMA wires will be able to provide recentering capabilities even when taken out to strain levels that would typically be associated with a seismic event.
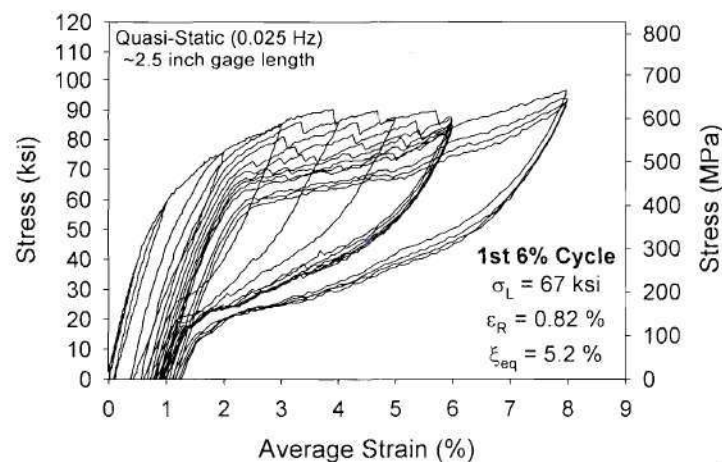

Figure 8: Stress-strain plot for a previously untested 2.16 mm (0.085 inch) diameter NiTi wire tested quasi-statically

A comparison can be made between the specimen which was tested "as is" from the manufacture (shown in Figure 8) and a specimen that was annealed at 350°C (662°F) for 30 minutes and then

immediately water quenched. As was previously mentioned, the loading protocol for the annealed specimen was implemented under strain control and strains were measured based on a 25.4 mm (1.0 inch) gage length extensometer as opposed to the specimen shown in Figure 8 which was run under displacement control with strains measured based on cross-head displacement. Figure 9 shows the stress-strain curve for the annealed 2.16 mm (0.085 inch) diameter NiTi wire specimen. The annealed specimen shows good superelastic properties with the formation of both the loading and unloading plateaus and the ability to return to its original undeformed shape. The loading plateau stress is not affected by the annealing of the specimen as the loading plateau stress values for the untreated and annealed specimen are 462 MPa (67 ksi) and 469 MPa (68 ksi), respectively. This results suggest that the load at which the phase transformation initiates is unaffected by prior heat treating of the specimens. A similar result can be seen for the unloading plateau stress value. The main advantage gained by first annealing the wire specimen is the decrease in the residual strain that is accumulated with continued cycling. The residual strain associated with the untreated and annealed specimens are 0.82% and 0.27%, respectively for the first 6% strain cycle. The annealed specimen provides a much better recentering capability than the untreated specimen which can be credited to the annealing process reducing any dislocations that may have formed in the material during previous processing and thus limiting the amount of permanent slip in the material before testing. Although annealing the specimen provided better recentering capabilities, there was a decrease in the equivalent viscous damping value from 5.2% for the untreated specimen to 3.03% for the annealed specimen for the first 6% strain cycle. The onset of strain hardening also occurred at lower strain levels for the annealed specimen, although this may be associated with the fact that the strain was measured using an extensometer rather than cross-head displacement which was used for the untreated specimen.
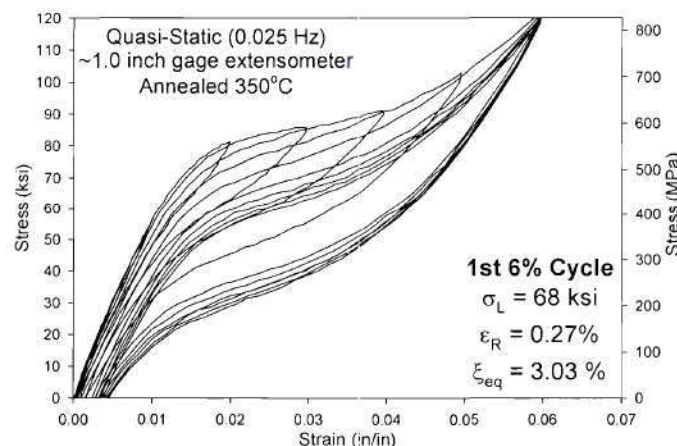

Figure 9: Stress-strain plot for a previously tested 2.16 mm (0.085 inch) diameter NiTi specimen which was annealed at 350°C (662°F) for 30 minutes and water quenched

Dynamic Test Results

The stress-strain results for the dynamic 0.5 Hz, 1.0 Hz, and 2.0 Hz wire tests are shown in Figure 10. As with the quasi-static test, the three plots show typical superelastic behavior with the formation of the loading plateau, unloading plateau, and only a small accumulation of residual strain providing an indication that larger diameter wires may be applicable for

earthquake engineering applications. The loading plateau stress increased with the increased strain rate from 462 MPa (67 ksi) for the quasi-static test to 476 MPa (69 ksi) for the 0.5 Hz strain rate to 496 MPa (72 ksi) for the 2.0 Hz strain rate at the first 6% strain cycle. More notably, the unloading plateau significantly increased with the increased strain rates. This can again be attributed to the self-heating of the wire specimen during the higher loading rates. Since the 2.16 mm (0.085 inch) diameter specimen is larger than the 0.254 mm (0.01 inch) diameter specimen, the self-heating had a larger effect on the unloading plateau as it became more difficult to dissipate the heat accumulated from the phase transformation. The significant increase in the unloading plateau stress led to a lowering of the equivalent viscous damping value for the first 6% cycle due to a pinching of the hysteresis with increased cycling rates. The equivalent viscous damping for the first 6% cycle was 2.99% and 2.11% for the 0.5 Hz test and the 2.0 Hz test, respectively. This result further suggests that superelastic NiTi shape memory alloys can only provide supplemental damping capacity, but cannot solely be used for energy dissipation in a structure under loading rates typical of an earthquake. Although the equivalent viscous damping detrimentally decreases with increased strain rate, the residual strain also decreases with increased strain rate leading to better recentering capability of the NiTi SMA wire under dynamic loadings. The residual strain for the first 6% cycle reduced from 0.79% to 0.60% for 0.5 Hz test and the 2.0 Hz test. This shows that the 2.16 mm (0.085 inch) diameter wires also maintain good recentering capabilities at strain rates and strain levels typically experienced by a building system during an earthquake.
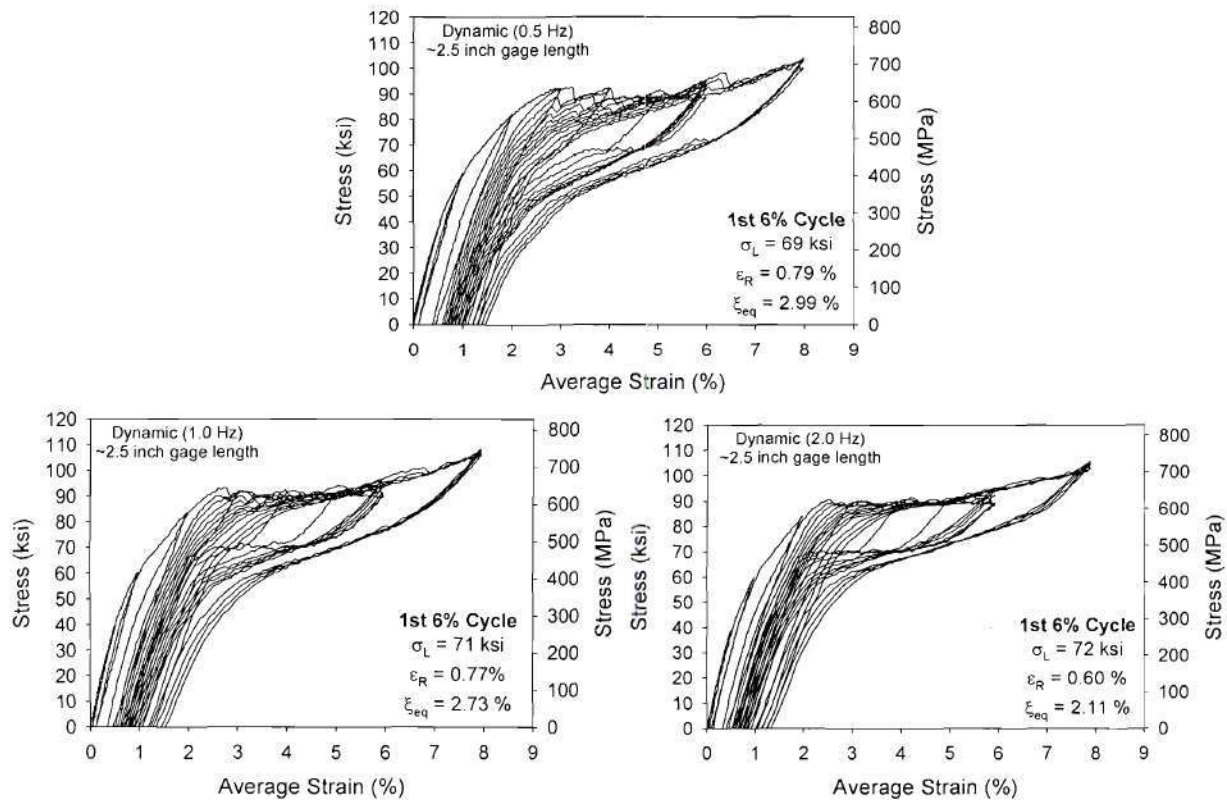

Figure 10: Stress-strain plot for a previously untested 2.16 mm (0.085 inch) diameter NiTi wire tested dynamically at 0.5 Hz, 1.0 Hz, and 2.0 Hz

Cyclic Properties Study

The plots shown in Figure 11 provide the initial elastic modulus, loading plateau stress, residual strain, and equivalent viscous damping values with respect to maximum cyclic strain for the 2.16 mm (0.085) inch diameter previously untested NiTi wires. The plots include the results from the quasi-static test and the dynamic tests at 0.5 Hz, 1.0 Hz, and 2.0 Hz. The initial elastic modulus is only shown up to the first 6% strain cycle in Figure 11(a) since the accumulation of the residual strain distorted the calculation of the initial elastic modulus which was measured as the slope of the loading curve from the start of a cycle to the point at which 1% strain was reached. The initial elastic modulus results show an initial increase in the elastic modulus followed by a decrease in the elastic modulus for the larger strain cycles. The elastic modulus for the quasi-static test had a larger final value and showed the largest variation in the elastic modulus with cycling as compared to the dynamically tested specimens. The specimen tested quasi-statically had an initial elastic modulus of approximately 44.8 GPa (6500 ksi) for the 2% strain cycle and an initial elastic modulus of approximately 52.1 GPa (7550 ksi) for the first 6% strain cycle. The dynamically loaded specimens all showed similar results with initial elastic modulus values typically remaining between 44.8 GPa (6500 ksi) and 51.7 GPa (7500 ksi).

Figure 11(b) shows the effect that loading rate and strain level had on stress at which the phase transformation from austenite to stress-induced martensite began. For all four strain rates, the loading plateau stress decreased with increased maximum cyclic strain and increased cycling. This can be attributed to localized slip assisting the phase transformation from austenite to stress induced martensite, particularly for the larger maximum strain levels. There is only a small difference between the loading plateau stress values for the four strain rates, but it is clear that increasing the strain rate leads to a decrease in the loading plateau stress. Comparing the results for the six 6% strain cycles, it is apparent that there is degradation in the loading plateau stress when cycled continually at a given strain level. It has been suggested that mechanically training shape memory alloys can reduce this degradation providing a more consistent behavior. If the specimens are not mechanically trained prior to implementation of the material into a structural system, the degradation of the loading plateau stress needs to be accounted for.

Figure 11(c) provides the residual strain values with respect to maximum cyclic strain and strain rate. The plot shows an increase in residual strain with increased cycling as a result of the formation of permanent localized slip which also affected the loading plateau stress values. The plots show a large increase in the residual strain value between the 1% strain cycle and 3% strain cycle. The increase between these strain levels was approximately 0.5% for all four strain rates where there was only a minor increase in the accumulation of residual strain between the 3% cycle and the first 6% cycle. The typical accumulation of residual strain during these intermediate cycles was typically less than 0.2%. The results also show a minor influence of strain rate on the accumulation of residual strain as the residual strain values decreased slightly with an increase in strain rate as was mentioned previously for the first 6% strain cycle. In all cases, the residual strain remained below 1.6% even after the specimens were cycled four times at 8% strain showing good recentering capability even at large strain levels typical of earthquake type loadings.

The variation in equivalent viscous damping with respect to maximum cyclic strain and loading rate can be seen in Figure 11(d). The plot shows a similar trend for all loading rates with increased strain level. The equivalent viscous damping values increased as expected for the 2% strain cycles as the specimens went from elastic to the onset of the phase transformation from austenite to stress-induced martensite. The specimens then provided a basically constant equivalent viscous damping value between the 2% strain cycle and 6% strain cycle. At the larger strain cycles (6% and 8%), the equivalent viscous damping values decreased as a result of strain hardening at the larger strain levels. The results show that damping is best provided when the specimens are cycled within their transformation plateau. With respect to strain rate, Figure 11(d) shows a large decrease between the equivalent viscous damping for the specimen tested quasi-statically and those tested dynamically. For the first 6% strain cycle, the equivalent viscous damping values for the quasi-static and 0.5 Hz tests were 5.22% and 2.99%, respectively. There was also a decrease from the 0.5 Hz tested specimen (2.99%) to the 2.0 Hz tested specimen (2.11%) for the first 6% strain cycle. The equivalent viscous damping value shows a clear decrease with increased strain rate which can be associated with the increase in the unloading plateau with increased strain rate mentioned previously. Once again, it is important to note that the equivalent viscous damping values for austenitic NiTi are low in general for damping applications.
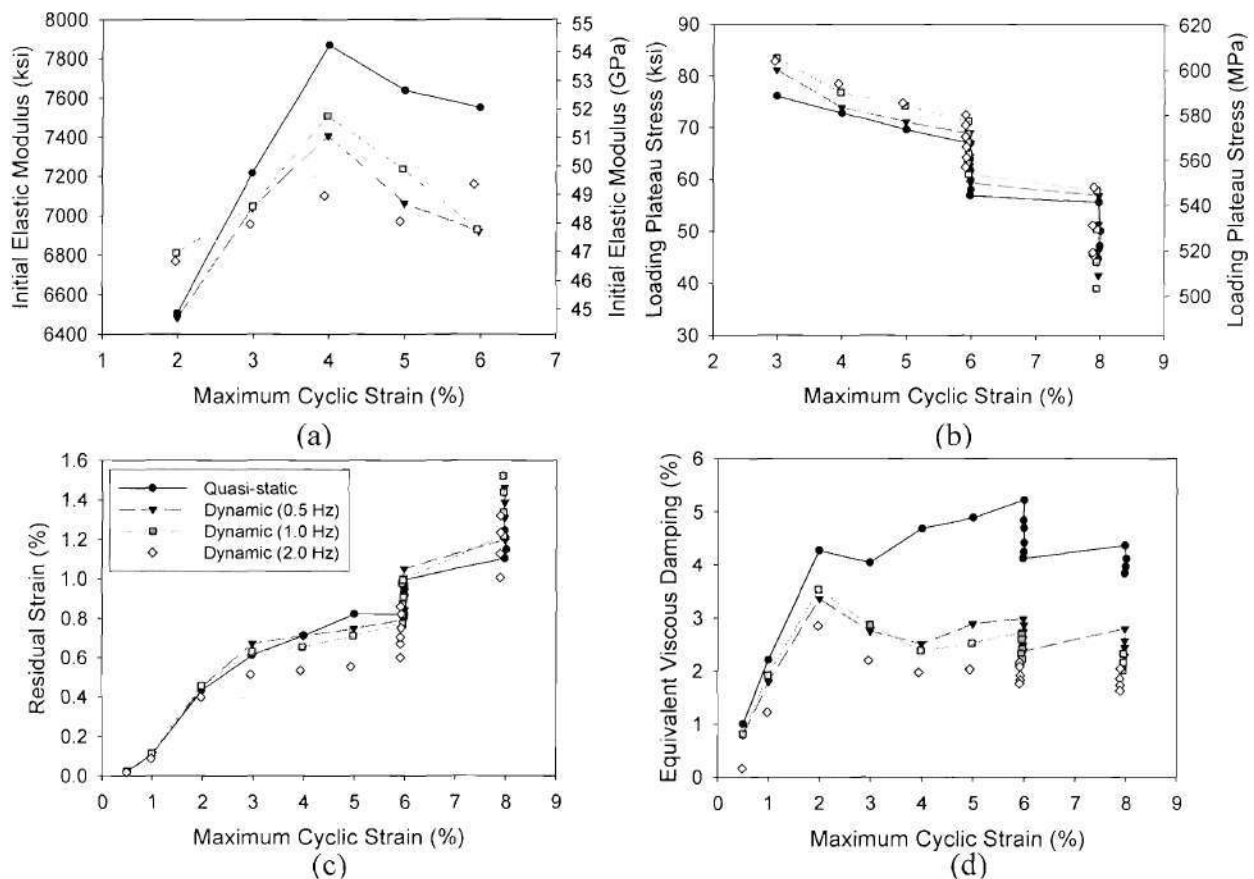

Figure 11: Comparison of NiTi 2.16 mm (0.085 inch) diameter wire subjected quasi-static and dynamic cyclic loading showing: (a) initial elastic modulus, (b) loading plateau stress, (c) residual strain, and (d) equivalent viscous damping

Comparison of the 0.254 mm (0.01 inch) and 2.16 mm (0.085 inch) Diameter Wire Results

In order to determine the optimal size wire for a particular SMA composite application, it is important that the differences in there mechanical behavior be studied. Comparing the quasi-static test results shown in Figure 3 and Figure 8, both size specimens provide good superelastic properties. The loading plateau stress for the larger diameter wire for the first 6% strain cycle is larger than that for the 0.254 mm (0.01 inch) diameter wire specimen, 531 MPa (77 ksi) and 462 MPa (67 ksi), respectively. Although, the smaller diameter wire provides lower residual strain values when cycled to the first 6% strain cycle showing better recentering capability. The dynamic plots for the two size wire specimens maintain the increased loading plateau for the larger diameter wire specimen. This increase may be attributed to the small cross-section of the 0.01 inch diameter wire where the formation of permanent slip may have a more profound effect on where the forward transformation stress occurs. The difference in the loading plateau stress may also be associated with small discrepancies in the composition of the two materials as these values were not supplied by the manufacturer and it is known that small changes in percentage of Ni in the specimen can produce large changes in the mechanical behavior of austenitic shape memory alloys. The main differences in the dynamic stress-strain plots for the 0.254 mm (0.01 inch) diameter wire shown in Figure 4 and those for the 2.16 mm (0.085 inch) diameter wire shown in Figure 10 is the amount in which the unloading plateau stress increased. There was a much larger increase in the unloading plateau stress for the larger diameter specimen as opposed to the 0.254 mm (0.01 inch) diameter specimen. As previously mentioned, this can be attributed to the ability of the smaller diameter wire to more efficiently dissipate the heat generated by the cycling at the higher loading rates.

Comparing the cyclic property plots shown in Figure 6 for the 0.254 mm (0.01 inch) diameter wires and those shown in Figure 11 for the 2.16 mm (0.085 inch) diameter wires, it is apparent that similar trends with respect to maximum cyclic strain for the initial elastic modulus, loading plateau stress, residual strain, and equivalent viscous damping values are obtained for the different size wires. This can more readily be seen in Figures 12 and 13 which depict the cyclic properties for the 0.254 mm (0.01 inch) diameter wire and the 2.16 mm (0.085 inch) diameter wire tested quasi-statically and dynamically at 1.0 Hz, respectively. The 2.16 mm (0.085 inch) diameter specimens had larger initial elastic modulus values as compared to the 0.254 mm (0.01 inch) diameter specimens. The initial elastic modulus values ranged between 22.1 GPa (3200 ksi) and 34.5 GPa (5000 ksi) for the smaller diameter specimens while the larger diameter specimens had initial elastic modulus values ranging between 44.1 GPa (6400 ksi) and 55.2 GPa (8000 ksi). Further, the initial elastic modulus for the 0.254 mm (0.01 inch) diameter specimens increased with an increased loading rate while the value decreased with increased loading rate for the 2.16 mm (0.085 inch) diameter specimens. Further work is needed to determine the reason for this occurrence.

The loading plateau stress for both the 0.254 mm (0.01 inch) diameter and 2.16 mm (0.085 inch) diameter specimens decreased with an increase in maximum cyclic strain and continued cycling. During dynamic testing, both size specimens showed a small increase of less than 34.5 MPa (5 ksi) in the loading plateau stress when cycled at higher strain rates. Similarly, the residual strain results for the 0.254 mm (0.01 inch) diameter and 2.16 mm (0.085 inch) diameter specimens were similar in that each increased with increasing strain cycles. However, the 2.16 mm (0.085

inch) diameter specimen did show a decrease in residual strain with increased strain rate while no real trend could be associated with the 0.254 mm (0.01 inch) diameter wire results. Overall, the residual strain values for both size specimens were similar and showed that both austenitic NiTi wires could be used for recentering applications.

A comparison of the equivalent viscous damping values for the 0.254 mm (0.01 inch) diameter and 2.16 mm (0.085 inch) diameter wires shows that while the damping values for the 0.254 mm (0.01 inch) diameter wires continue to increase with increased cycling, the damping attributed to the 2.16 mm (0.085 inch) diameter wires plateaus during the intermediate strain cycles and decreases at larger strain levels. The equivalent viscous damping values for both size specimens decreased with increased strain rate as a result of the increase in the unloading plateau at higher strain rates and the subsequent reduction of the hysteretic area. In general, the damping values for both size wires remained below 6% suggesting that austenitic NiTi wire specimens cannot be used in purely damping applications.
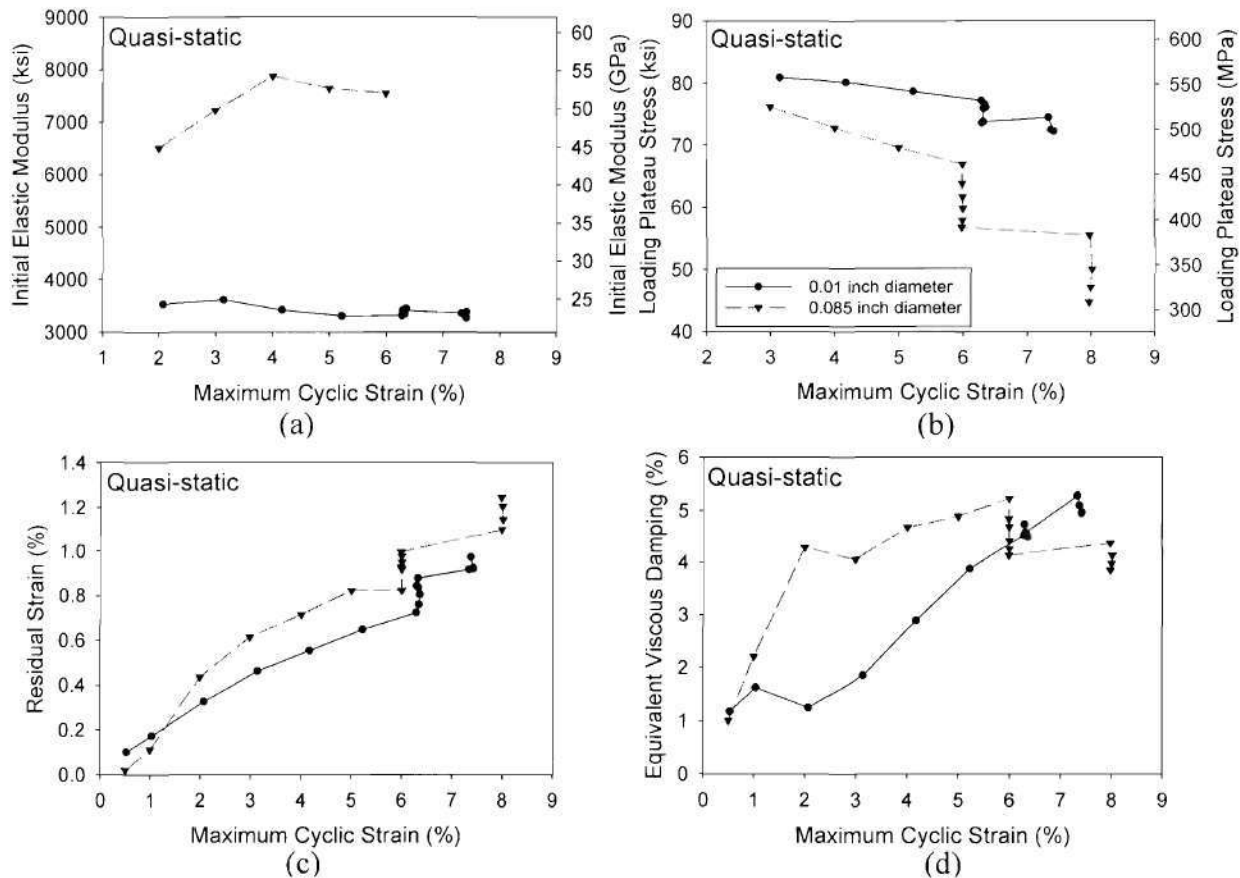

Figure 12: Comparison of the NiTi 0.254 mm (0.01 inch) and 2.16 mm (0.085 inch) diameter wire subjected quasi-static cyclic loading showing: (a) initial elastic modulus, (b) loading plateau stress, (c) residual strain, and (d) equivalent viscous damping
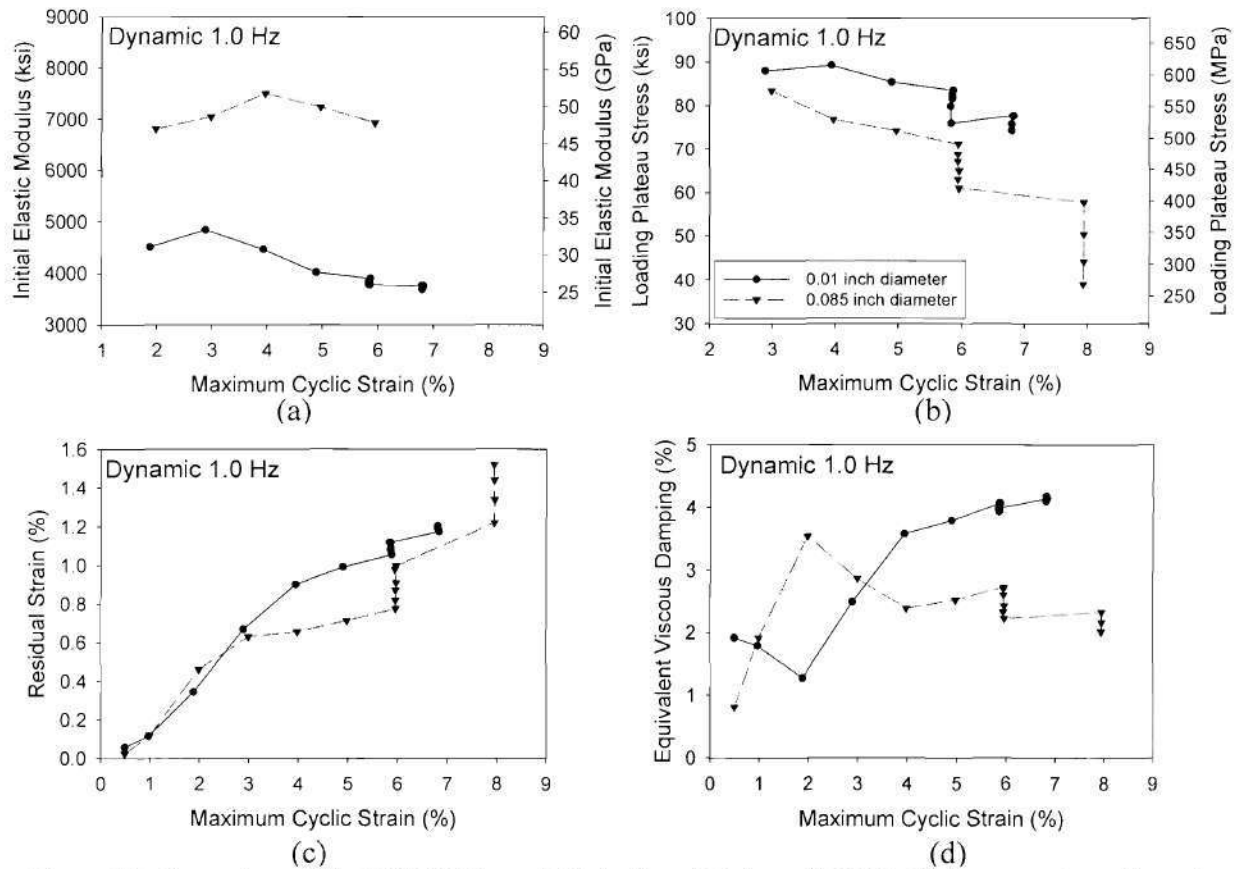
Figure 13: Comparison of the NiTi 0.254 mm (0.01 inch) and 2.16 mm (0.085 inch) diameter wire subjected dynamic (1.0 Hz) cyclic loading showing: (a) initial elastic modulus, (b) loading plateau stress, (c) residual strain, and (d) equivalent viscous damping

Both sizes of wires show good superelastic properties which would be beneficial in seismic design and retrofit applications. They provided good recentering capability, formation of loading plateaus, and some damping which would tend to reduce the response of a structure during an earthquake. By using these size specimens as fibers in a polymer matrix composite system, further benefits of added damping, strength, and buckling restraint may be obtained which would further optimize the beneficial superelastic NiTi shape memory alloy properties.

Summary of Key Findings and Recommendations

The austenitic NiTi wires studied looked at the behavior of two sizes (0.254 mm (0.01 inch) and 2.16 mm (0.085 inch) of NiTi SMA wires to determine how the mechanical properties of each are effected by wires size and cycling at rates and levels consistent with those expected during a seismic event. The tests were conducted on previously untested NiTi wires which all had an austenite start temperature below room temperature ensuring that the wires would have superelastic properties when tested. A far field type loading protocol consisting of increasing strain cycle was applied under displacement control both quasi-statically and dynamically in order to evaluate the cyclic properties of both size wires. The initial elastic modulus, loading

plateau stress, unloading plateau stress, residual strain, and equivalent viscous damping values were compared to determine whether strain rate, strain level, or specimen size affected the mechanical behavior under tensile loading and were used to determine the plausibility of using NiTi SMAs as fibers in a polymer matrix composite system for earthquake engineering applications.

Both size specimens showed good superelastic properties when cycled quasi-statically. The larger diameter specimens typically provided larger initial elastic modulus values, equivalent viscous damping values, and residual strain values. Although, the smaller diameter wire specimens provided a higher stress to initiate the phase transformation suggesting a larger initial elastic zone. The trends associated with increased cycling and increased strain level were similar for both sizes of wires with a decrease in the initial elastic modulus and loading plateau stress when cycled at increased strain levels, which can be associated with the formation of permanent localized dislocations.

As was seen for the quasi-static tests, the wires cycled dynamically showed good superelastic properties with a minor distortion to the unloading plateau. Similar trends as with the specimens tested quasi-statically were found where the larger diameter wires provided larger initial elastic modulus values and lower loading plateau stresses. For the dynamic tests though, the residual strains for the smaller specimens were higher. This can be attributed to an increase in residual strain with increased cycling rate for the smaller diameter specimens, which is opposite of what has previously been found in past studies suggesting minor slipping at higher loading rates. Equivalent viscous damping values were also higher for the smaller diameter specimens because of their ability to dissipate generated heat more efficiently.

Further tests showed that cycling specimens more than once through the loading protocol resulted in more stable properties and lower residual strain values for subsequent tests. This result suggests the possibility of mechanically training specimens before implementing them into applications to ensure more consistent and desirable properties. Annealing studies also showed that the residual strain and equivalent viscous damping values could be optimized based on the annealing temperature and annealing time.

The results suggest the use of austenitic NiTi SMAs as fibers in polymer matrix composite systems is possible provided adequate bonding is present. The NiTi SMAs will provide a unique recentering capability which will act as a prestressing force on the composite material while the matrix of the composite will provide added damping and some buckling constraint when cycled in compression. It is further suggested that the NiTi SMA wires be annealed prior to being implemented into the composite in order to optimize the recentering (residual strain) properties. Prior mechanical training would also provide a composite with more consistent properties. Given the more consistent behavior of the 2.16 mm (0.085 inch) diameter wires, the larger diameter wires are recommended, although the smaller diameter wires (0.254 mm (0.01 inch)) can provide more flexibility and with proper annealing and training may provide composites with desired properties.

2. SHAPE MEMORY ALLOY COMPOSITES

As the use of shape memory alloys in structural and seismic applications continues to be explored and gain acceptance, methods of implementing them into structures need be developed. Typically, earthquake engineering applications would require large diameter specimen in order to provide the desired stiffness to the structure and adequate stress plateaus to limit the amount of force transferred to other members of the structure during a seismic event. One possible solution is to introduce the shape memory alloys into structural bracing systems or other recentering and damping applications as the fibers of a composite material. The use of shape memory alloys as fibers in a polymer matrix composite allows for the use of smaller diameter SMA wires which are typically manufactured for current use in biomedical, commercial, and aerospace applications. The use of shape memory fibers will, in concept, provide the recentering capability, hysteretic energy dissipation, and low- and high-cycle fatigue properties associated with shape memory alloys, which have previously been shown, while also providing some buckling constraint and further energy dissipation due to the confinement and deformation of the composite matrix material. Testing of single shape memory alloy wires has been previously presented, but further testing of the composite specimens must be undertaken in order to ensure that the composite specimens provide the desired mechanical behavior which is indicative of a single SMA wire specimen, namely good recentering capabilities and energy dissipation.

Polymer Matrix Composites with 2.16 mm (0.085 inch) Diameter NiTi Fibers

Test Specimens

Two sets of composite specimens were tested during this study. The first set consisted of 15.9 mm (0.625 inch) diameter composite specimens of length 356 mm (14 inches). The second set of specimens consisted of 15.9 mm (0.625 inch) diameter composite specimens with lengths of 406.4 mm (16 inches). The first set of test specimens were used in order to perfect the grip fixture for tensile loadings and perform cyclic compressive tests while the second set of test specimens were used to perform cyclic tensile tests at various strain rates. Both sets of specimens used 30 2.16 mm (0.085 inch) diameter NiTi wires as unidirectional fibers held together by a polymer matrix. The specimens were encased in Adiprene and an O-ring cord stock was used for the core. The same size and composition NiTi wires which were tested previously are used as the fibers with no additional annealing or processing of the NiTi shape memory alloys being performed.

Loading Protocol

Since the composite specimens were studied to determine their potential use in earthquake engineering applications, a loading protocol simulating typical strain levels and strain rates of a far field type earthquake was used. Because the extensometer could only be placed on the outer Adiprene surface, all tests were run in displacement control. The strain levels for the loading protocol were determined based on the cross-head displacement and a gage length of 152.4 mm (6 inches). The resulting far field type loading protocol consisted of strain cycles of 0.5%, 1.0%-5% by increments of 1%, and two cycles to 6.0%, 8.0%, 10.0%, 12.0%, 14.0%, and 16.0%, respectively. A typical plot of the loading protocol can be seen in Figure 12. Given the inability

to accurately determine the gage length due to the complexity of the grip fixture and motion within the load train, the strain values calculated based on the cross-head displacement tended to overestimate the strains obtained from the extensometer readings. The first set of tensile tests was run quasi-statically at a loading rate of 0.025 Hz. Dynamic tests were then run in order to simulate loading rates typical of a seismic event. These tests were performed at both 0.5 Hz and 1.0 Hz. The compressive tests performed on the shorter specimens used the same loading protocol, but placed the specimen into compression rather than tension. Compression tests were only run quasi-statically at a controlled displacement rate of 1.27 mm/min (0.05 in/min) and the extensometer was not used to measure strain values. Strains for the compression test were calculated based on cross-head displacement with a gage length of approximately 152.4 mm (6 inch).
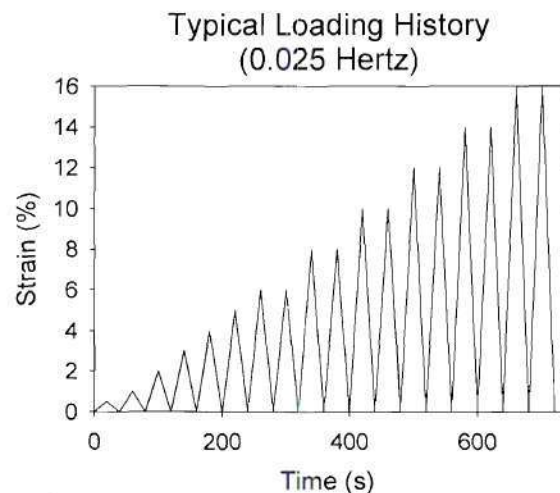
Typical Loading History (0.025 Hertz)

Figure 12: Typical quasi-static loading protocol for cyclic tensile testing of the 15.9 mm (0.625 inch) diameter composites

Experimental Test Setup

The same 250 kN (55 kip) MTS hydraulic testing apparatus was used to perform tests on both sets of 15.9 mm (0.625 inch) diameter composite specimens. Special grips were fabricated in order to properly grip the composite specimens and provide a uniform distribution of the load through the cross-section of the composite. As was mentioned previously, the loading protocol was run in displacement control based on the loading protocol shown in Figure 12, but all strain measurements reported for the tensile tests will be based on the extensometer attached to the outer Adiprene surface. Both the specimens used for compression (shorter) and the specimens used for tension had a gage length of approximately 152.4 mm (6 inches). For the tensile specimens, the Adiprene surface and composite material needed to be removed from the NiTi wires for a length of 127 mm (5 inches) at each end of the composite in order to allow for proper gripping of the specimen. Figure 13 shows a picture of the two sizes of round specimens used. The loading protocol was input using an MTS TestStar controller running *TestWare* software, which used the cross-head displacement feedback to control the actuator. Force limits were also placed on the loading protocol to limit the amount of compression the tensile specimen underwent and to limit the amount of tension that the compression specimen underwent. All tests were performed on previously untested composite specimens with each loading rate being

performed on a single specimen due to limited materials. The extensometer used to measure strain had a gage length of 25.4 mm (1 inch). The residual strain, loading plateau stress, initial elastic modulus, and equivalent viscous damping were used to evaluate the behavior of the 15.9 mm (0.625 inch) diameter composite specimens which contained 30 unidirectional NiTi wire fibers.
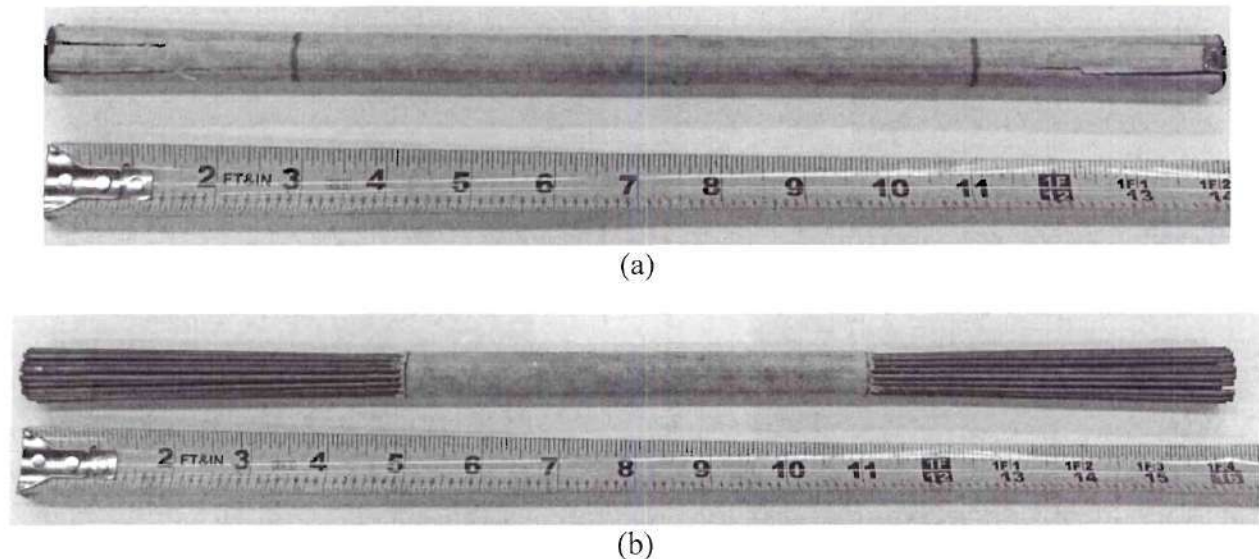

(a)

(b)

Figure 13: The 15.9 mm (0.625 inch) diameter composite specimens of length (a) 356 mm (14 inches) and (b) 406.4 mm (16 inches) prior to testing (the longer specimen has the composite material removed from the ends

Quasi-static Test Results

The stress-strain curve for composite specimen R3-2 (15.9 mm (0.625 inch) diameter and length 406.4 mm (16 inches)) is shown in Figure 14. Approximately 45% of the cross-sectional area of the specimen is made up of 2.16 mm (0.085 inch) diameter NiTi superelastic SMA wires. The stress-strain results show a clear flag shape hysteresis suggesting that composites which contain approximately half volume percentage of NiTi provides similar mechanical behavior as single wire NiTi superelastic specimens. The typical loading plateau and unloading plateau associated with superelastic shape memory alloys is formed with a small amount of strain hardening present at the larger strain cycles. The loading plateau stress decreases from 359 MPa (52 ksi) for the first cycle greater than 4% strain to 317 MPa (46 ksi) for the last cycle of the loading protocol. This result suggests that the use of shape memory alloys in composites does not effect the degradation of the loading plateau stress typically associated with single wire NiTi specimens. The unloading plateau stress also decreases with continued cycling, but to a much lesser extent as compared with the loading plateau. The equivalent viscous damping reaches a maximum of approximately 4.4%, which occurred during the 4.85% strain cycle. The results suggest that more composite material is necessary in order to provide larger amounts of damping capacity. Large damping capacities would be necessary in order to make shape memory alloy composites suitable for use in purely damping seismic applications in structures. Only slight changes occurred in the initial elastic modulus with continued cycling suggesting that only small amounts of permanent slip are occurring in the shape memory alloy fibers and that the composite material only contributes minimally to the stiffness of the material. Most importantly, the shape memory alloy composite specimen showed good recentering capabilities even when cycled to 6% strain.

The maximum residual strain remained below 0.47%. This suggests that the composite specimens with NiTi shape memory alloy wire fibers can provide recentering capabilities even when taken out to strain levels that would typically be associated with a seismic event and compare similarly to the behavior typically seen of single wire or single bar shape memory alloys specimens.
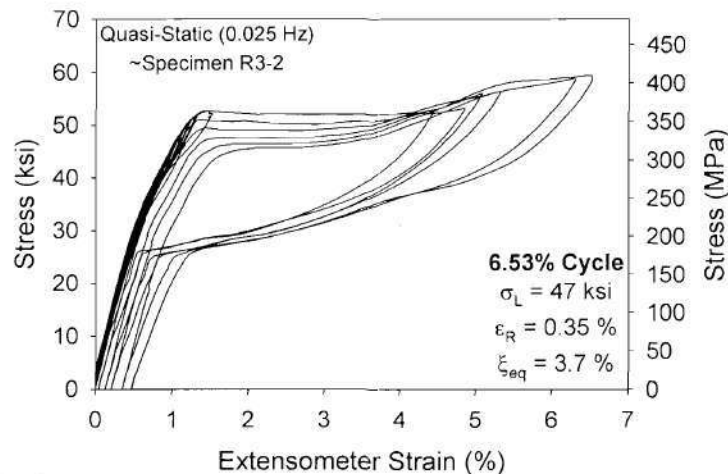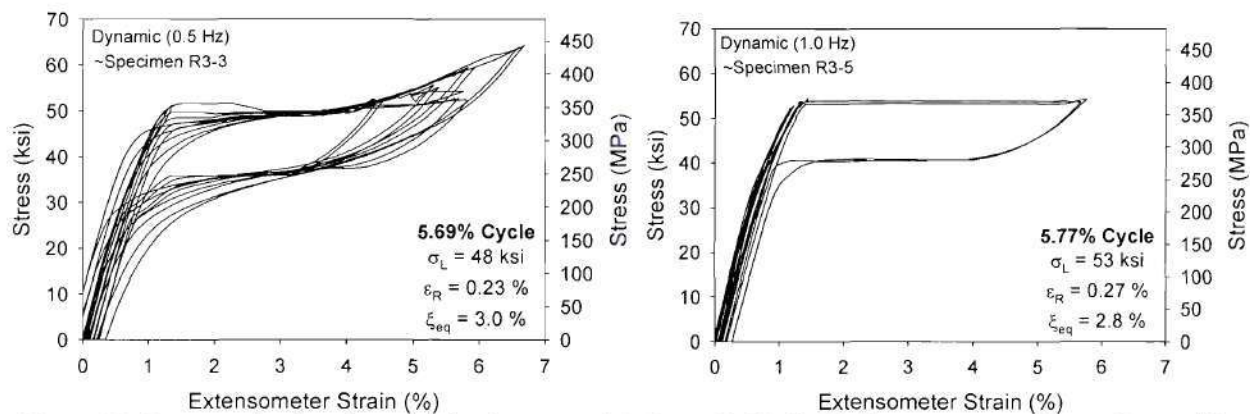

Figure 14: Stress-strain plot for a previously untested 15.9 mm (0.625 inch) diameter composite specimen with a length of 406.4 mm (16 inches) tested quasi-statically (45% NiTi SMA)

Dynamic Test Results

The stress-strain results for the dynamic 0.5 Hz and 1.0 Hz (specimens R3-3 and R3-5) composite tests conducted on the 15.9 mm (0.625 inch) diameter, 406.4 mm (16 inches) length specimens are shown in Figure 15. During testing, there was a small amount of slip with the extensometer during the 0.5 Hz test after the second cycle over 6% strain. The 1.0 Hz test only has two cycles above 6.0% strain due to a failure of the composite specimen during testing as a result of the Adiprene sheath surrounding the NiTi wires splitting. Both dynamic stress-strain curves show similar superelastic behavior as was seen in Figure 14 with the composite specimen tested quasi-statically. Both plots show a clear loading and unloading plateau with good recentering capabilities indicating that composite specimens with NiTi fibers perform well under typical earthquake loading rates. The results show a small increase in the loading plateau stress with the increased strain rate. The quasi-static test resulted in a loading plateau stress of approximately 329 MPa (47.7 ksi) for the 5.1% strain cycle where the loading plateau stress increased to approximately 331 MPa (48.0 ksi) and 365 MPa (53 ksi) for the 0.5 Hz and 1.0 Hz loading rates, respectively. The small increase in the loading plateau stress compared to that typically associated with single wire specimens may be attributed to the matrix material preventing self-heating of the NiTi wires at higher loading rates. The dynamic tests also show an increase in the loading plateau at higher loading rates leading to a decrease in the maximum equivalent viscous damping value with increase loading rate. The maximum equivalent viscous damping decreased from approximately 4.4% for the quasi-static specimen to 3.2% for the specimen tested at 0.5 Hz and 2.8% for the specimen tested at 1.0 Hz. The test further suggest the needed for added matrix material in order to provide more energy dissipation during cycling as it has been shown that superelastic NiTi wires alone cannot provide enough damping capacity to be used in purely damping seismic applications. The recentering capacity of the composite

specimens increased with increased strain rate as is shown by the decrease in the accumulation of residual strain when cycled out to high strain levels. This result suggests that composite specimens would work well in seismic recentering applications and actually would perform better under the rates typically associated with an earthquake loading. The maximum residual strain decreased from approximately 0.47% for the quasi-static test to approximately 0.27% for the dynamic 1.0 Hz test. The stress-strain curves show that composite specimens provide similar mechanical behavior as compared to single wire NiTi specimens and maintain good recentering capabilities at strain rates and strain levels typically experienced by a structural system during an earthquake.

Figure 15: Stress-strain plots for a previously untested 15.9 mm (0.625 inch) diameter composite specimen with a length of 406.4 mm (16 inches) tested dynamically at 0.5 Hz and 1.0 Hz (45% NiTi SMA)

Cyclic Properties Study

The plots shown in Figure 16 provide a comparison of the initial elastic modulus, loading plateau stress, residual strain, and equivalent viscous damping values with respect to maximum cyclic strain for the 15.9 mm (0.625 inch) diameter composite specimens with lengths of 406.4 mm (16 inches). The results are shown for the quasi-static, 0.5 Hz, and 1.0 Hz test in order to provide a means of comparing those properties important for seismic applications with respect to strain level and strain rate. As was previously mentioned, there was a small amount of slip with the extensometer during the 0.5 Hz test. The data resulting from cycles after the extensometer slip has been removed from these plots for accuracy purposes. Due to testing the specimens in displacement control, the maximum cyclic strain tended to decrease during consecutive cycles to the same strain level. This can be attributed to small amounts of slipping in the grips and the accumulation of residual strain. Neither occurrence affects the overall trends associated with the results.

The initial elastic modulus with respect to maximum cyclic strain and loading rate is shown in Figure 16 (a). All three loading rates show a similar trend with increased maximum cyclic strain. The initial elastic modulus decreases until the maximum cyclic strain is large enough to initiate the martensitic phase transformation at which point the initial elastic modulus tended to increase slightly with increased strain levels. The initial decrease in the elastic modulus can be attributed to slip and a slight break down in the microstructure during initial cycling. The later increase in the initial elastic modulus can be associated with the formation of permanent deformation which

tends to limit the movement of the microstructure and stiffen the material. A clear strain rate effect on the initial elastic modulus exists. The initial elastic modulus has higher values for higher loading rates and shows a larger initial decrease when cycled quasi-statically. The specimens had and initial elastic modulus of 29.9 GPa (4300 ksi) for the 5.32% strain cycles when cycled quasi-statically which increased to 33.1 GPa (4800 ksi) for the 5.69% strain cycle and 34.2 GPa (4970 ksi) for the 5.67% strain cycle when cycled at 0.5 Hz and 1.0 Hz, respectively. The results show an increased stiffness of the composite specimens at high loading rates, but a decrease in the initial stiffness with continued cycling which would tend to result in a change in the natural frequency of the structure during a seismic event.

The effect that loading rate and strain level have on the loading plateau stress of the composite specimen containing 2.16 mm (0.085 inch) diameter NiTi fibers is shown in Figure 16(b). The results are only shown for cycles which reached a maximum cyclic strain greater than 4.0% as the lower cycles did not show evidence of the initiation of the thermoelastic martensitic phase transformation. As a result, only two points were obtained for the 1.0 Hz specimen. The results show a decrease in the loading plateau stress with increased strain level during cycling. Previous work has shown this occurrence to be attributed to the formation of localized slip which tends to assist the forward transformation process. The quasi-static and dynamic 0.5 Hz results provide similar loading plateau stress values, while the dynamic 1.0 Hz results provide a significantly higher value for the loading plateau stress. The plots suggest that at moderate loading rates, the composite matrix material may act to help dissipate the heat resulting from the exothermic-endothermic phase transformation. Although at loading rates of 1.0 Hz and higher, the added heat can not be dissipated fast enough even with the composite matrix material resulting in a self-heating of the NiTi fibers and an increase in the loading plateau stress typically associated with cycling shape memory alloys at higher temperatures. The use of more thermally conductive matrix material and higher volume percentages of matrix material may provide a means of stabilizing the loading plateau stress with continued cycling.

As is typical of materials containing shape memory alloys, Figure 16(c) shows an increase in the residual strain with increased maximum cyclic strain. This increase in residual strain with continued cycling can also be attributed to the formation of permanent localized slip and permanent dislocation which locally inhibit the reverse transformation from stress-induced martensite back to the initial austenitic structure. The 1.0 Hz specimen shows a larger initial increase in the residual strain, but a much smaller maximum residual strain. The results show an over all decrease in the maximum residual strain value with increased cycling rate. The maximum residual strain for the quasi-static, dynamic 0.5 Hz, and dynamic 1.0 Hz tests were approximately 0.47%, 0.35%, and 0.27%. All three of these values remained below 1% even when cycled to strain levels as high as 6.5%. The composite specimens all showed good recentering capabilities and the capability to be used in seismic applications as recentering devices.

Figure 16(d) provides the variation in equivalent viscous damping for the composite specimen containing NiTi wire fibers with respect to maximum cyclic strain and loading rate. The plot shows similar trends for all loading rates where the equivalent viscous damping values tend to increase until the 4%-5% strain cycles and then decrease for larger strain cycles. This decrease can be associated with a pinching of the hysteresis with continued cycling and strain hardening

associated with the completely stress-induced martensitic phase leading to a decrease in the hysteretic area. The results show that damping is best provided when the specimen is cycled to strain levels within the loading plateau. The plots also show a clear effect of strain rate on the equivalent viscous damping value. Cycling at quasi-static loading rates provide higher maximum equivalent viscous damping value, approximately 4.43%, as compared to cycling dynamically at 0.5 Hz or 1.0 Hz, 3.2% and 2.8%, respectively. The decrease in the equivalent viscous damping values can be attributed to the significant increase in the unloading plateau during high strain rate cycling as a result of a self heating of the specimen. This increase in the unloading plateau stress leads to a pinching of the hysteresis and an overall decrease in the hysteretic area during dynamic cycling. One possible way to add damping capacity to the composite specimen would be to add a higher volume percentage of matrix material which produces a larger hysteresis. Although, a balance must be obtained between increased damping capacity and loss of recentering capability as the increased amount of matrix material would tend to also increase the residual strain values during cycling. In general, it is important to note that austenitic NiTi shape memory alloys alone typically have damping values too low to be used in purely damping seismic applications.
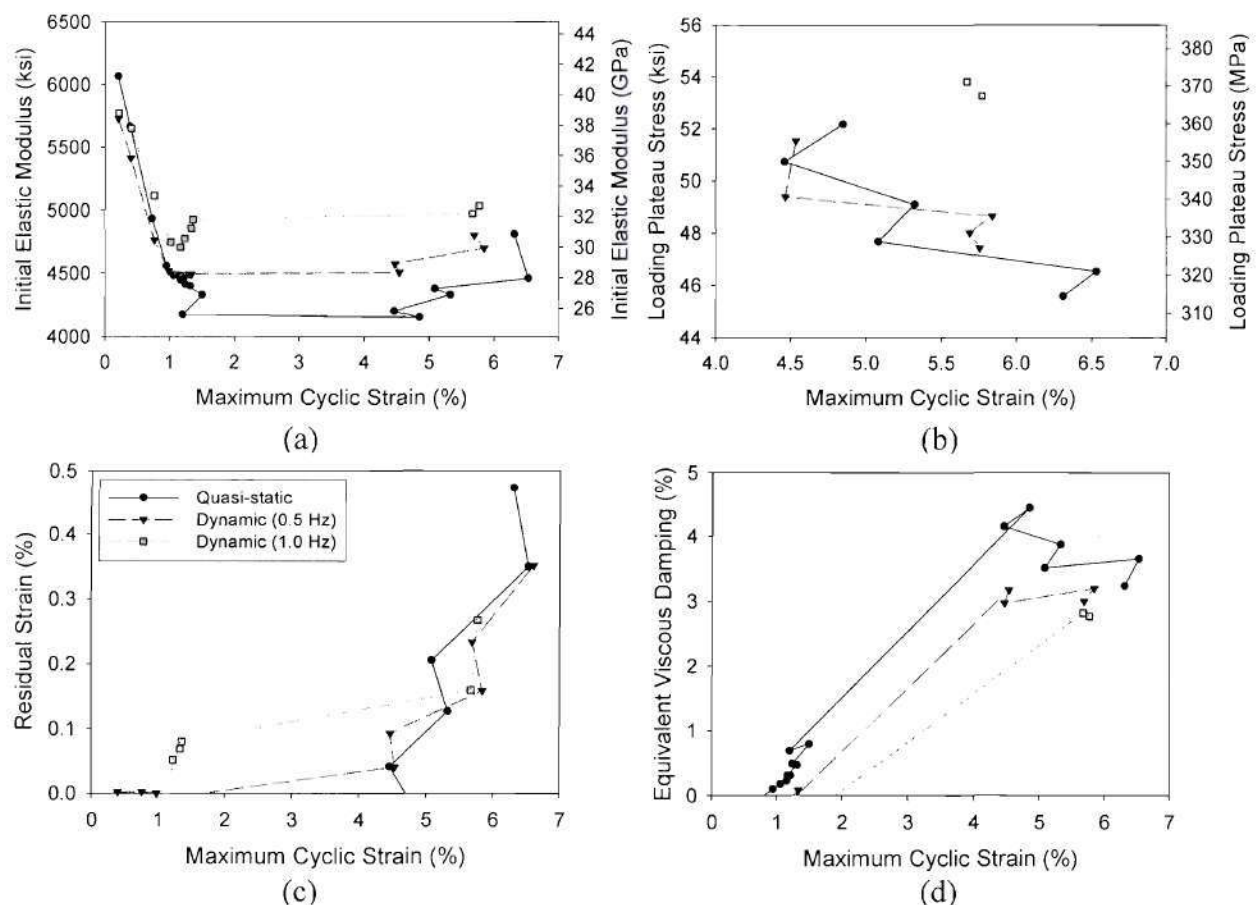

Figure 16: Comparison of NiTi 15.9 mm (0.625 inch) diameter composite with NiTi fibers subjected to quasi-static and dynamic cyclic loading showing: (a) initial elastic modulus, (b) loading plateau stress, (c) residual strain, and (d) equivalent viscous damping

Compression Test Results

A15.9 mm (0.625 inch) diameter composite specimens of length 356 mm (14 inches) was used to perform a cyclic compression test. As with the tensile specimens, the compressive specimen contained 30 austenitic NiTi 2.16 mm (0.085 inch) diameter wires which made up the unidirectional fibers of the composite. The composite specimen was not restrained from buckling and had an approximate gage length of 160 mm (6.3 inches). The strain was measured based on cross-head displacement as the grip fixtures did not allow adequate space to attach an extensometer when testing in compression.

The resulting stress-strain curve for the cyclic compressive test is shown in Figure 17. The test was stopped after the -4% strain cycle due to the large horizontal deflection of the specimen during buckling which was causing an interaction between the specimen and the grip fixture at high strain levels. The specimen remained within the elastic range up to the 1% strain cycle. Upon reaching a strain level of approximately 1.3% and a corresponding stress of approximately 131 MPa (19 ksi), the specimen underwent buckling. After buckling, the composite specimen showed good shape recovery with residual strains remaining below 0.5% even after being cycled to -4% strain. Even under compressive loads and buckling, the NiTi fibers provide good recentering capabilities to the composite material. Both before and after buckling, the compressive stresses remain considerably smaller than those associated with the tensile specimens suggesting a limited force transfer to other members of the structure. The stress-strain curve does maintain the hysteretic behavior during cycling suggesting that composite specimens using NiTi fibers may be able to provide supplemental energy dissipation capacity when cycled in compression even upon undergoing buckling. The results further suggest the ability to use shape memory alloy composites in both a tensile and compressive capacity as opposed to just tensile applications which have been the focus of past research on single wire and thin plate austenitic shape memory alloys.
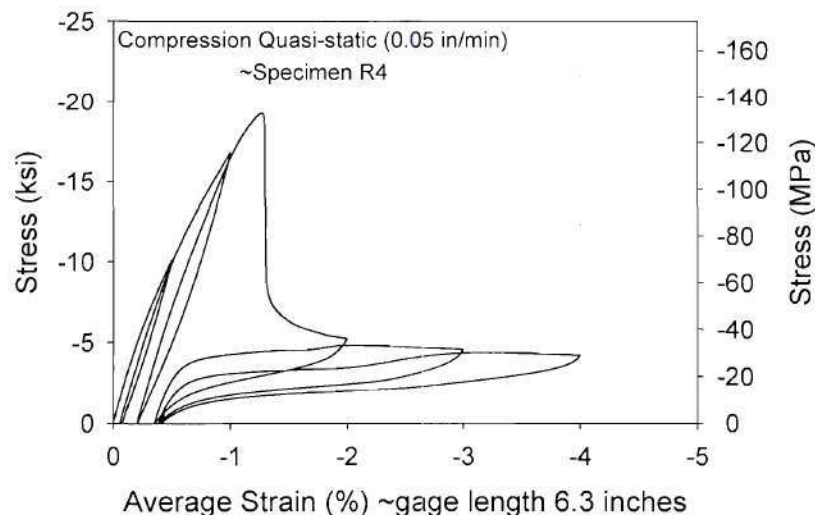

Figure 17: Compressive stress-strain plot for a previously untested 15.9 mm (0.625 inch) diameter composite specimen with a length of 356 mm (14 inches) tested at a loading rate of 1.27 mm/min (0.05 in/min) with 45%vol NiTi SMA unidirectional fibers

Compression Cyclic Properties

The plots shown in Figure 18 provide the initial elastic modulus, residual strain, and equivalent viscous damping values with respect to maximum cyclic strain for the 15.9 mm (0.625 inch) diameter composite specimen with unidirectional NiTi wires as fibers within the matrix. The loading plateau stress was not measured since the specimen underwent buckling before the -2% strain level could be reached. The initial elastic modulus was only measured up until the 2% strain cycle at which point the specimen buckled. The results shown in Figure 18(a) provide a consistent initial elastic modulus with continued cycling at increasing strain levels. There difference between the elastic modulus between the 0.5%, 1.0%, and 2.0% strain cycle remains below 3 GPa (435 ksi) suggesting that the stiffness provided to the structure under small compressive loadings will remain constant. The results further suggest that a consistent initial stiffness of a structure incorporating shape memory alloy composites may be able to be obtained under compressive loadings when the composites are restrained from buckling even at higher strain levels. Further work would need to be conducted with constrained compressive tests in order to ensure this behavior.

Figure 18(b) provides the residual strain values with respect to maximum cyclic compressive strain. The plot shows an increase in residual strain with increase compressive cycling. Although, the maximum residual strain associated with the -4% strain cycle was only 0.4% showing that even under compression, shape memory alloy composites can provide good recentering capabilities. The results also show a decrease in the rate at which the residual strain is accumulated with increased maximum cyclic strain, particularly after buckling has occurred. This behavior can be attributed to the fact that a large amount of the deformation is a result of the specimen bending rather than being compressed, which limits the amount of permanent deformation occurring in the NiTi fibers as some of the fibers are then being placed in tension while others are being placed in compression.

Figure 18(c) shows the variation in equivalent viscous damping with respect to maximum compressive cyclic strain. The equivalent viscous damping values tend to be larger than those associated with tensile specimens. The large equivalent viscous damping value obtained for the compressive 2% strain cycle is a result of the specimen buckling providing a much larger area under the curve before the buckling actually occurred and a much smaller stress value at the peak strain level as a result of the specimen buckling. If this large peak is ignored, the maximum equivalent viscous damping value obtained was approximately 6.4% during the -3% strain cycle which is about 2% higher than the maximum value obtained during tensile testing. The results suggest that under compressive loadings, shape memory alloy composites can provide higher damping capacity than under typical tensile loading. Further work needs to be done in order to confirm this result when compressive composite specimens are further confined from buckling. Overall, the compressive results show promise for implementing shape memory alloy composites into not only tensile seismic application, but also into compressive recentering and damping applications.
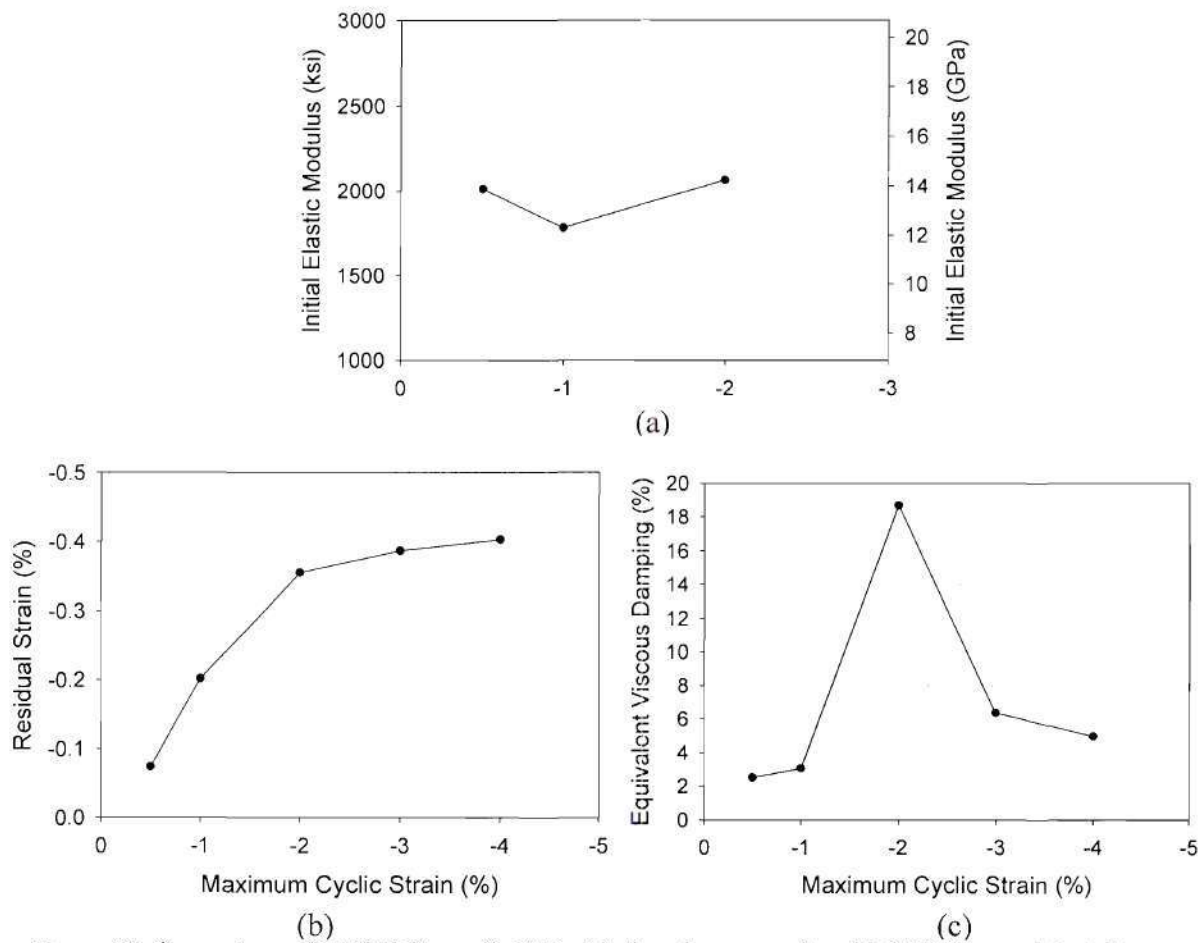
Figure 18: Comparison of NiTi 15.9 mm (0.625 inch) diameter composite with NiTi fibers subjected to a quasi-compressive cyclic loading showing: (a) initial elastic modulus, (b) residual strain, and (c) equivalent viscous damping

3. ANALYTICAL APPLICATIONS OF SHAPE MEMROY ALLOY COMPOSITES

Background

The unique ability of shape memory alloys to provide both recentering and damping capabilities has led to the possibility of using the material in seismic resistant design and retrofit of structures. Recent studies have shown that shape memory alloys can improve the seismic performance of both buildings and bridge systems. Baratta and Corbi (2002) found that superelastic shape memory alloys effectively attenuated the dynamic response of a simple portal frame system. A further study by Han et al. (2003) looked at the damping characteristics of shape memory alloys by studying the free vibration response of a reduced-scale steel frame with superelastic braces. These studies have given some validity to the use of shape memory alloys for seismic resistant design and retrofit, but have focused only on small scale and numerical models. Very little has been done in terms of how to implement shape memory alloys into actual building systems and their use in seismic resistant design and retrofit. One innovative way to obtain the benefits of both the recentering and damping capabilities of shape memory alloys is to implement them into structures as composites. By using shape memory alloys in the form of a composite, a larger area of shape memory alloys, which is needed for structural applications, can be obtained while still using the less expensive wire form of the shape memory alloy. A further advantage to using composite shape memory alloys is that the matrix helps to confine the shape memory alloy wires where a wound cable cannot. This will allow the shape memory alloy composite braces to resist compressive forces as well as tensile forces by restraining the wires from buckling.

3-Story Steel Frame

Model Characteristics

In order to determine the effectiveness of using composite shape memory alloy braces in seismic resistant design and retrofit of buildings, a nonlinear time history analysis is run on a 3-story steel structure utilizing two different bracing configurations: conventional steel square tube sections and composite shape memory alloy braces made up of shape memory alloy wires imbedded in a polymer matrix. The structure can be seen in Figure 19, where only one braced bay was studied due to the symmetry of the structures. Figure 20 shows how the composite shape memory alloy specimens are implemented into the bracing system. The composite shape memory alloy braces are modeled so as to provide the same axial stiffness and yield strength as the steel braces resulting in the two structures having the same natural period. In order to meet these restrictions, the required area and length of the composite shape memory alloy specimens were determined and it was assumed that these composite specimens would be connected to the frame by rigid segments in order to ensure that all deformation occurs in the composite shape memory alloy.

Earthquake Records

A suite of twenty records representing 10% probability of exceedance in 50 year ground motions for the downtown Los Angeles area was used to study the structure. The ground motions were scaled to the average spectral acceleration of all twenty ground motions at the fundamental

period of the structure. In order to quantify the results of the study and determine whether the shape memory alloy composite bracing system performed better than the conventional steel bracing system, the inter-story drifts and residual drifts of the top floor were compared.
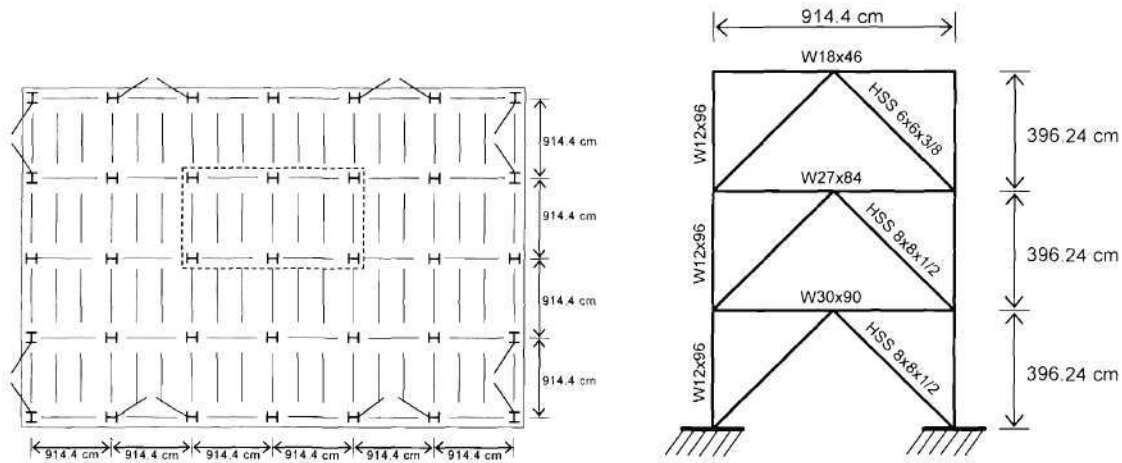

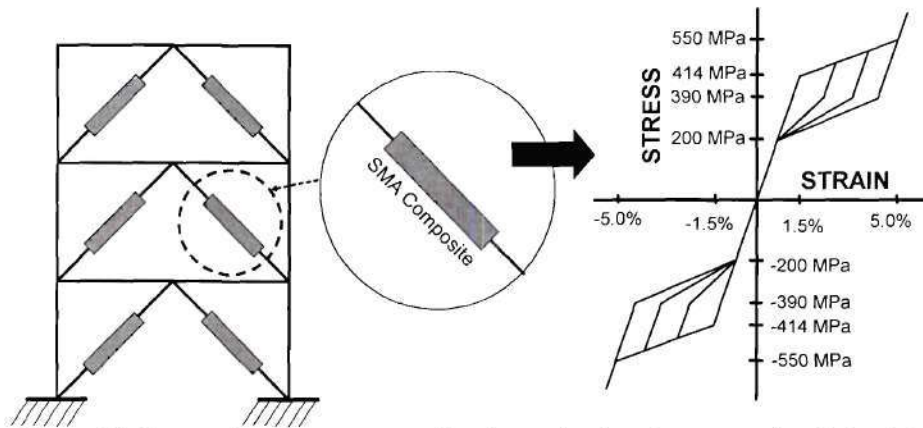**Figure 19:** Plan (left) and elevation (right) of the 3-story steel frame

Figure 20: Composite shape memory alloy brace detail and stress-strain relationship

Numerical Results

The maximum inter-story drift and residual drift of the top floor are traditionally used to evaluate the performance of a building during a seismic event. Both the conventional steel braced structure and the shape memory alloy composite braced structure have the same natural period resulting in both structures undergoing the same spectral accelerations. This allows for a comparison between the performances of each of the systems. The time history for the upper left node of the structure for each of the bracing systems can be seen in Figure 21 for the La14 scaled ground motion. The plot clearly shows a reduction in the displacement of the top floor with the use of shape memory alloy composite braces, which can be attributed to the ability of the composite shape memory alloys to recover their shape resulting in little or no residual strain with continued cycling. The shape memory alloy composites also increased the speed at which the vibration in the structure attenuated due to the damping capability of the composite. The shape

memory alloy composite braced structure showed a significant reduction in residual drift as compared to the steel braced structure as well.
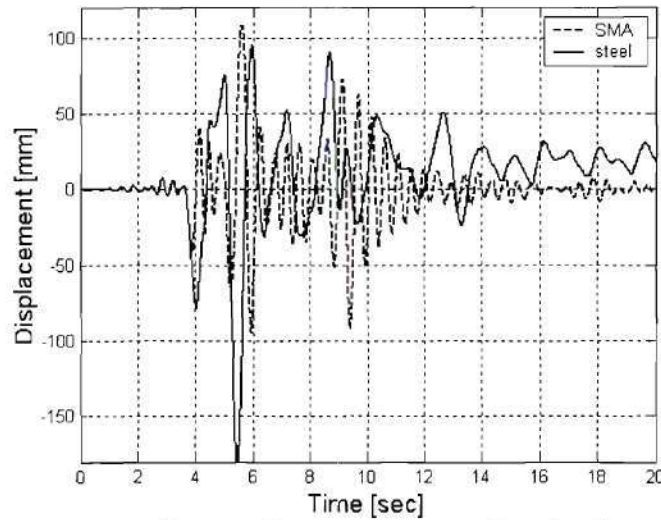

Figure 21: Displacement time-history of the 3-story frame undergoing the scaled La14 record

Figure 22 and 23 provide a comparison of the maximum inter-story drift values and residual drift values associated with all twenty scaled ground motions for both the conventional steel braced structure and the composite shape memory alloy braced structure. The results clearly show that the unique properties of the shape memory alloy composites reduce the inter-story drift values and help to decrease the accumulated permanent deformation in the steel frame after a seismic event. The ability of the shape memory alloy composites to resist buckling, while the conventional steel braces buckle in compression, allows for much lower displacement values in the shape memory alloy composite braced structure.
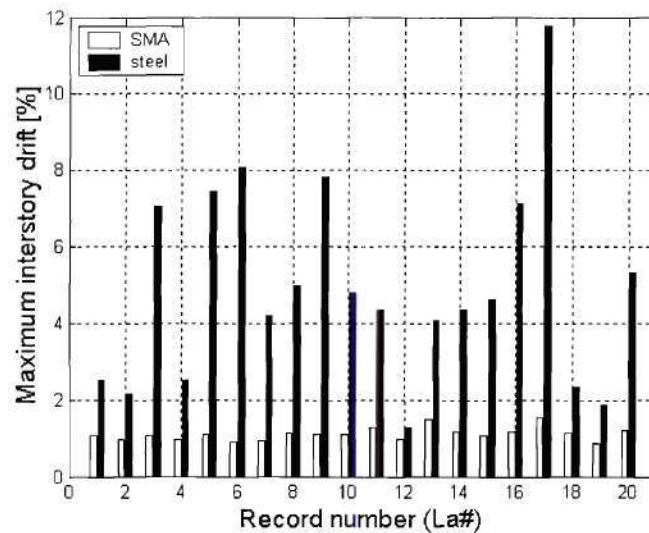
Figure22: Maximum inter-story drift exhibited by the 3-story frame equipped with either conventional or composite shape memory alloy braces
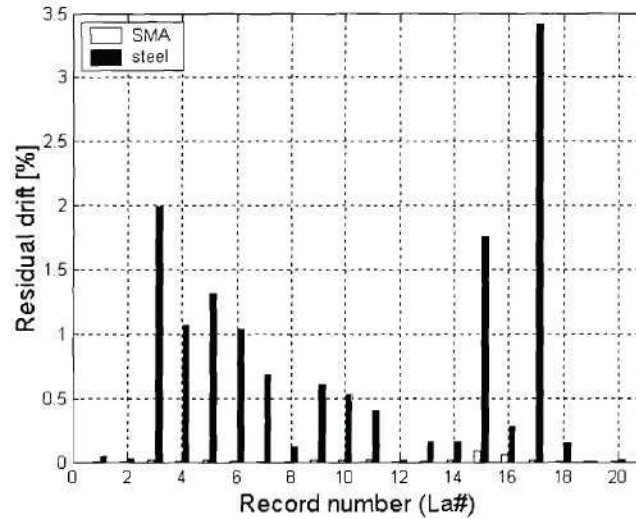
Figure 23: Residual drift exhibited by the top floor of the 3-story frame equipped either with conventional or composite shape memory alloy braces

Summary

The results show the effectiveness of using a composite shape memory alloy bracing system for seismic design and retrofit of structures. The large reduction in maximum inter-story drift values and accumulated residual drift as compared with conventional steel braces would reduce the damage imparted to a building structure and provide a structure that is more resistant to the occurrence of aftershocks. The ability of the composite system to use shape memory alloys wires in order to provide a substantial effective area of shape memory alloy material and also restrict buckling of the shape memory alloy wire provides a cost effective and optimal design and retrofit strategy as was demonstrated in the nonlinear time history analysis. This also suggests that further work looking at different configurations of composite shape memory alloy bracing systems and better characterization of the materials behavior can lead to the future implementation of shape memory alloy composites in structures and an ultimate decrease in the damage to such structures during and earthquake.

Section 3 References

A. Baratta and O. Corbi, "On the dynamic behavior of elastic-plastic structures equipped with pseudoelastic SMA reinforcements", *Computational Materials Science*, Vol. 25, 2002, pp. 1-13.

Y-L. Han, Q. S. Li, A-Q. Li, A. Y. T. Leung and P-H. Ling, "Structural vibration control by shape-memory alloy damper", *Earthquake Engineering and Structural Dynamics*, Vol. 32, 2003, pp. 483-494.
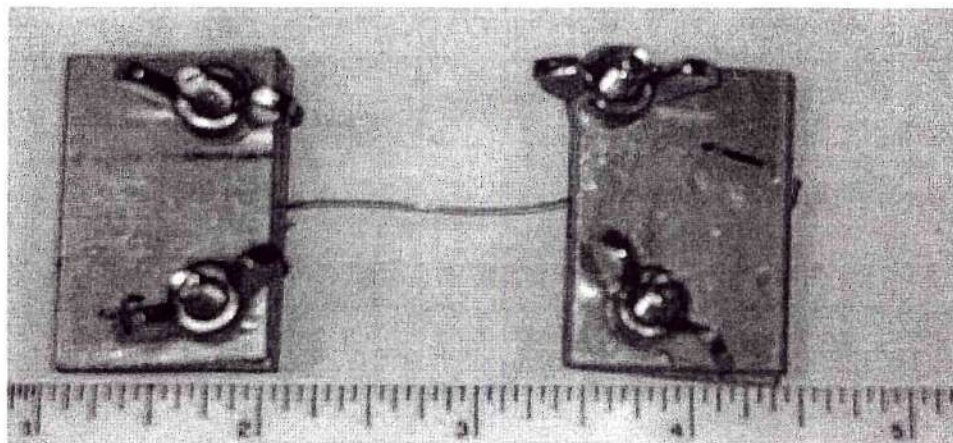
0.01" Diameter NiTi Wire Test Results

Test Specimens and Loading Protocol

A number of 0.01" diameter superelastic NiTi wires were tested in this study in order to determine the cyclic properties of the small diameter wire which will be used as fiber reinforcement in flat polymer matrix composite systems. All specimens were manufactured in the same batch and were tested as received from the manufacturer. No further annealing or processing was applied before testing. The loading protocol used to test the wire specimens consisted of increasing strain cycles of 0.5%, 1.0-5% by increments of 1%, six cycles at 6%, and four cycles at 7%. The first set of tests was run quasi-statically at a loading rate of 0.025Hz. Dynamic tests were then performed at 0.5Hz, 1.0Hz, and 2.0Hz. Each dynamic specimen was tested under the loading protocol three subsequent times without regripping of the specimen. With each test, the crossheads were adjusted such that there was no slack in the wire and the displacement and loads were reset to their zero levels accordingly.
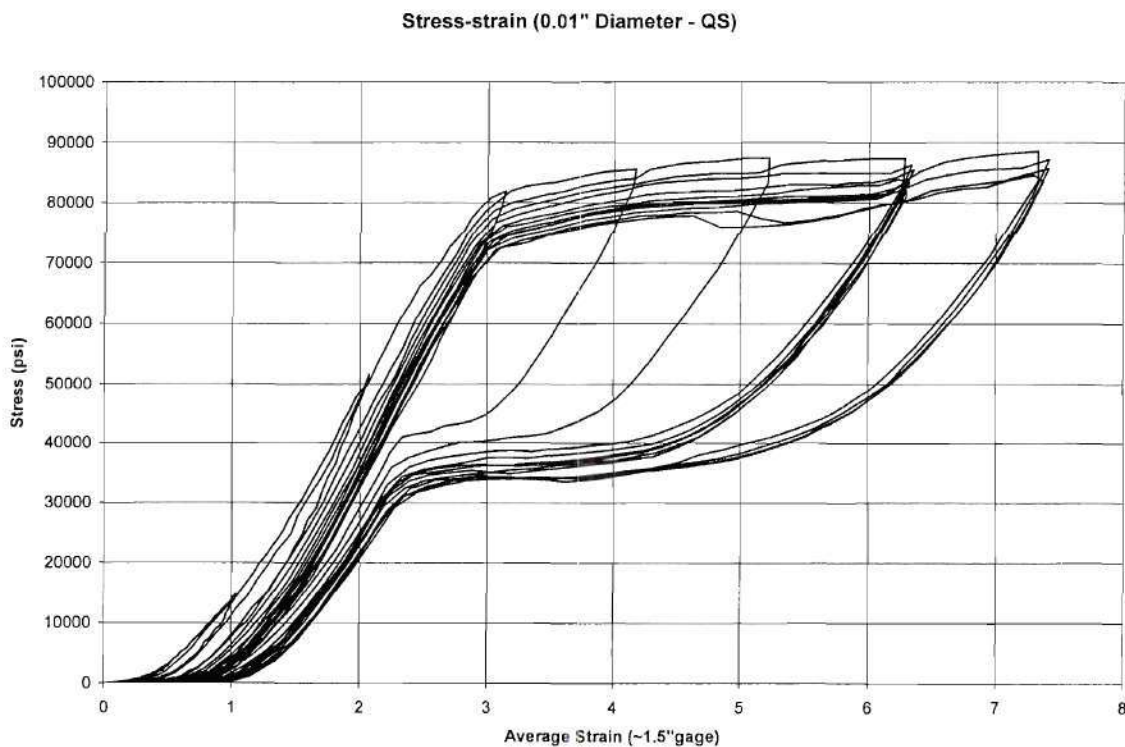
Experimental Setup

Testing of the 0.01" diameter specimens was done using an ELF 3200 Testing apparatus which consists of an electromagnetic actuator and a stroke capacity of 0.5 inches. The wire specimens were compressed between two aluminum plates and held in place with two screws and epoxy (see below) in order to limit slipping and facilitate gripping the specimens with the ELF 3200 DMA grip fixtures. The specimens had a gage length of approximately 1.5 inches. The loading protocol was run in displacement control with strain being measured based on cross-head displacement since the wires were too thin in order to facilitate the use of an extensometer. Wintest software was used in order to apply the loading protocol and acquire the data output. An 11 lbf load cell was used in order to measure the load on the specimen during testing.
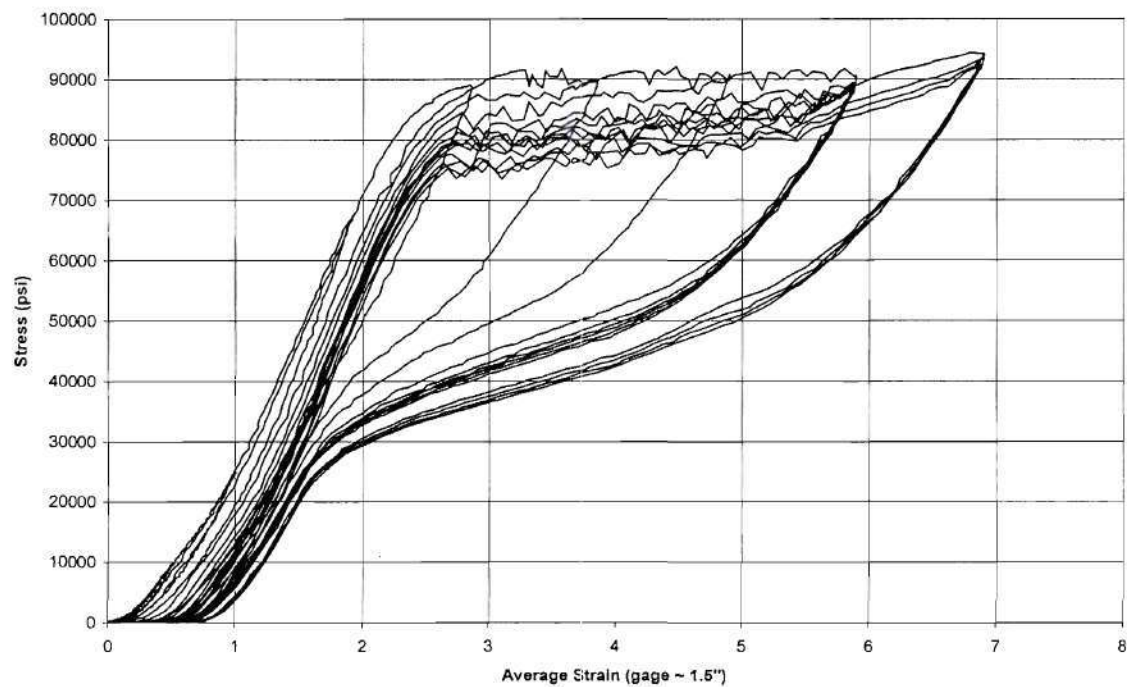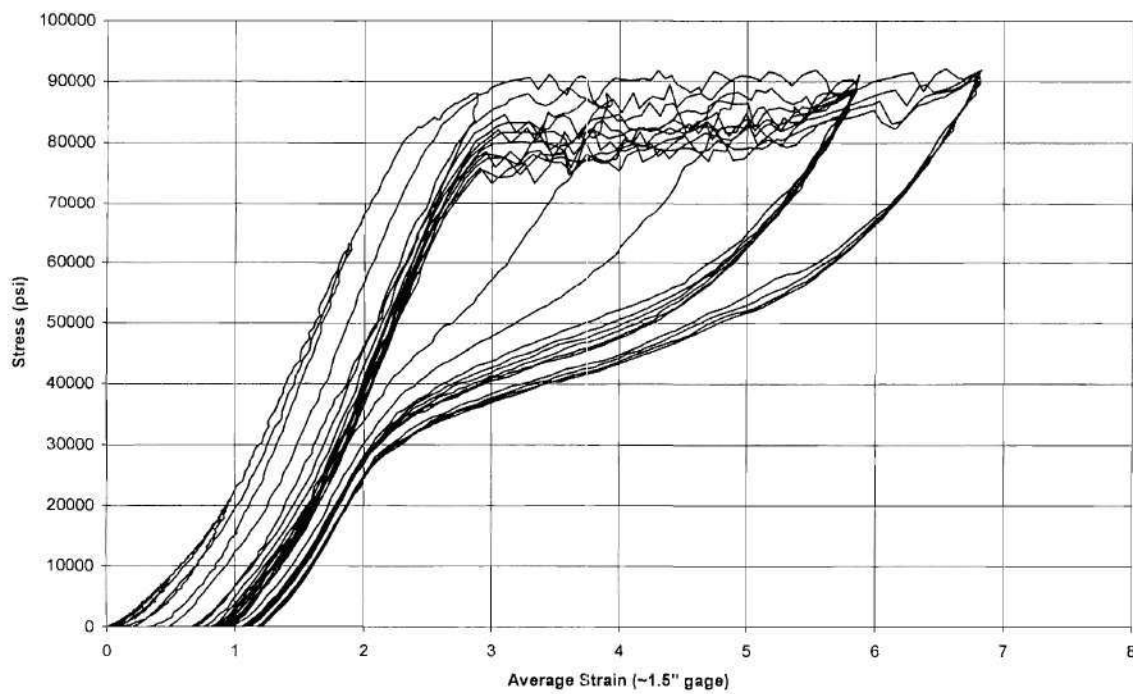
Stress-Strain Results

The stress-strain result for the untested 0.01" diameter superelastic NiTi wires run quasi-statically and dynamically at 0.5 Hz, 1.0 Hz, and 2.0 Hz are shown below. The plots show good superelastic behavior at all loading rates. The quasi-static plot appears to be shifted to the right suggesting possible slack or a small amount of initial slipping which may have occurred during the first loading cycle. This suggests that the residual strain and maximum strain values may be smaller than those obtained during this test. Differences in the maximum strain levels with each cycle can be attributed to small differences in the gage lengths when measured with a digital caliper. Each of the four sets of plots show loading plateaus of approximately 80 ksi. The unloading plateau was less defined with increased loading rate suggesting that a self-heating of the material is interfering with the reverse transformation since at the faster loading rates the specimen does not have time to dissipate the heat produced by the exothermic-endothermic phase transformation. Residual strain values remained below 1.4% for all loading rates providing good recentering capabilities even at high strain levels. There was a small decrease in hysteresis with increased loading rate due to an increase in the unloading plateau with an increase in loading rate at the larger strain levels, although all specimens maintained some hysteric damping capabilities.
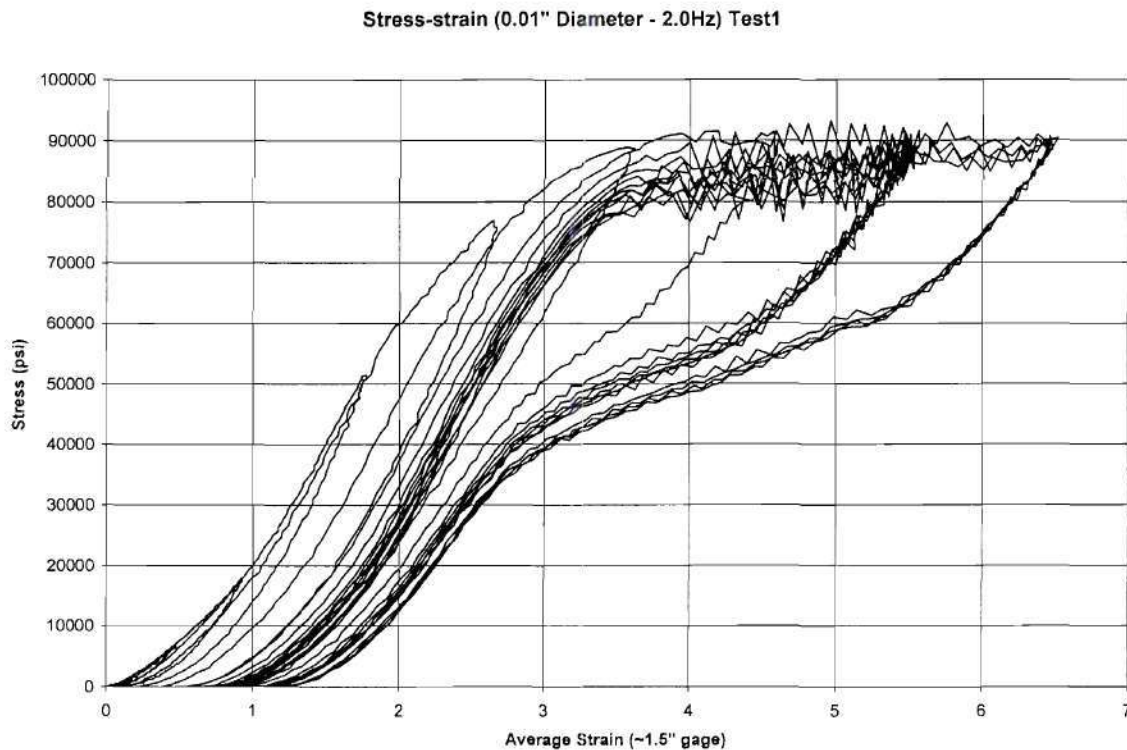
Stress-strain (0.01" Diameter - QS)

Stress-Strain (0.01" Diameter - 0.5Hz) Test 1

Stress-Strain (0.01" Diameter - 0.5Hz) Test 1

Stress-strain (0.01" Diameter - 1.0Hz) Test1

Stress-strain (0.01" Diameter - 1.0Hz) Test1

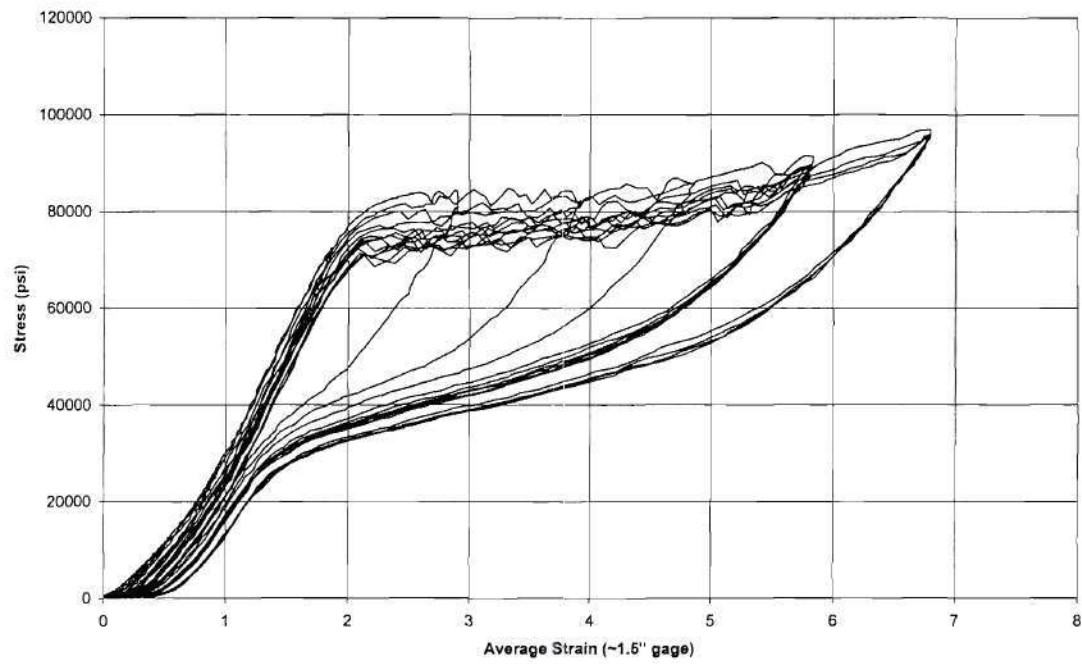**Stress-strain (0.01" Diameter - 2.0Hz) Test1**

Dynamic Stress-Strain Results

The second and third test of each of the dynamically cycled wires showed an interesting stabilization of the properties which can be seen in the stress-strain plots below of the wire specimen tested at 1.0 Hz for a second and third time. The rate of increase in residual strain shows a decrease during the second and third tests of the wire with the maximum value below 0.5% strain for the third test. The loading plateau and unloading plateau stabilized as well with the second and third tests suggesting that continued cycling of NiTi wire can help to stabilize the properties.

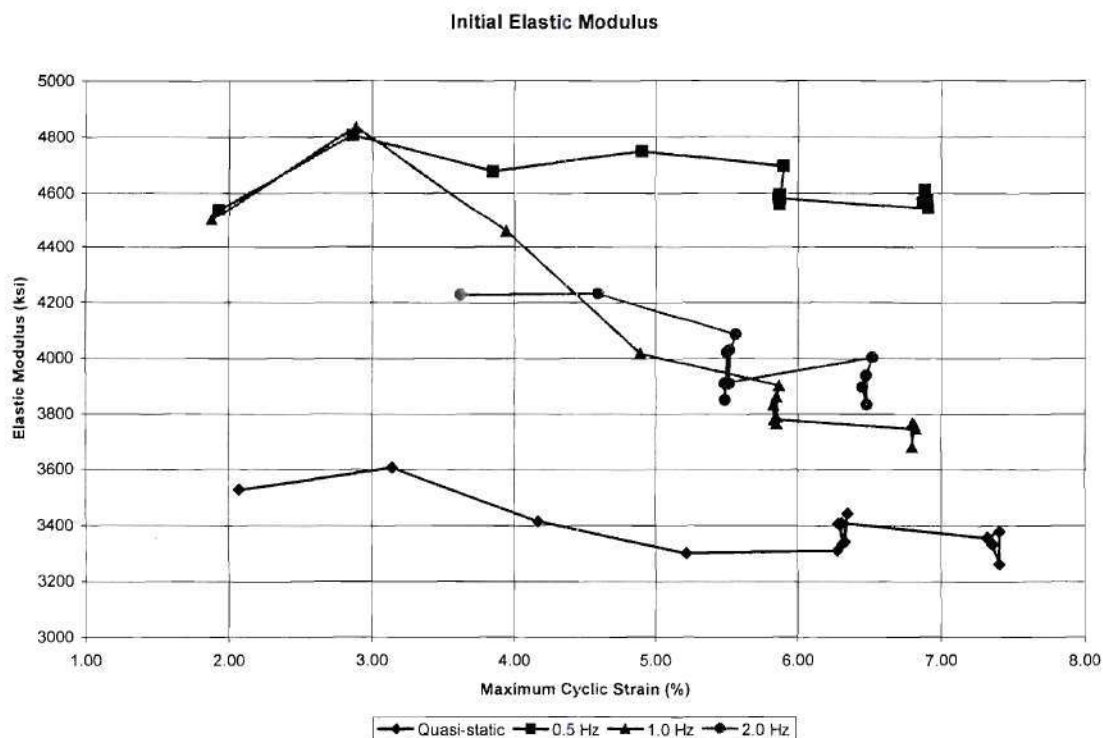**Stress-strain (0.01" Diameter - 1.0Hz) Test2**

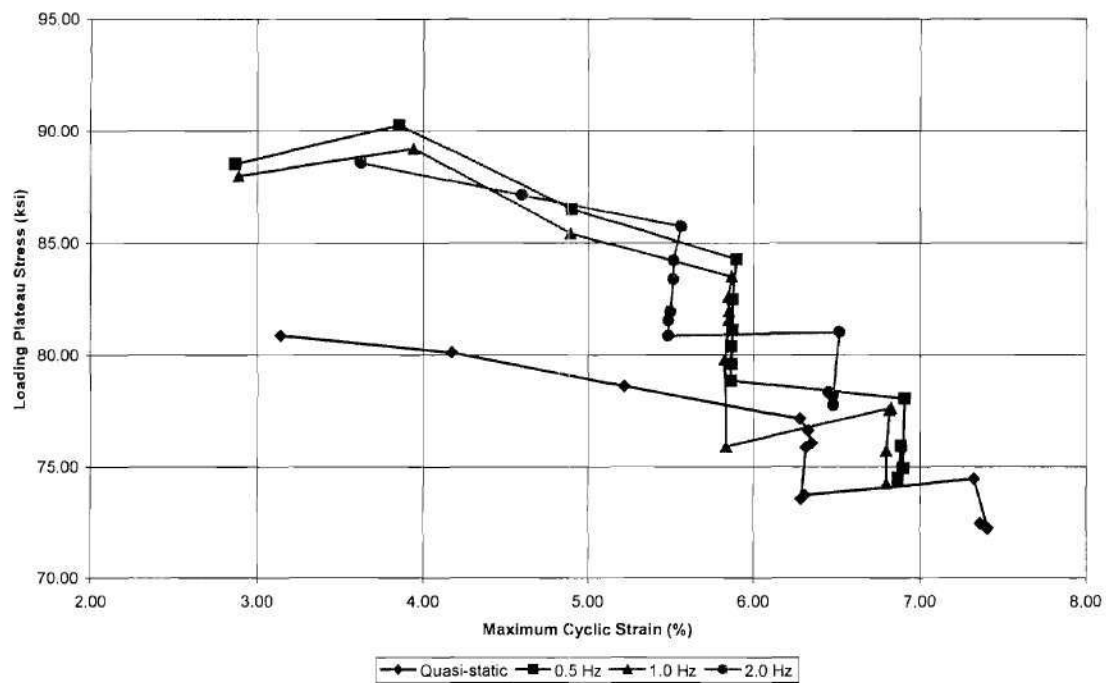**Stress-strain (0.01" Diameter - 1.0 Hz) Test3**
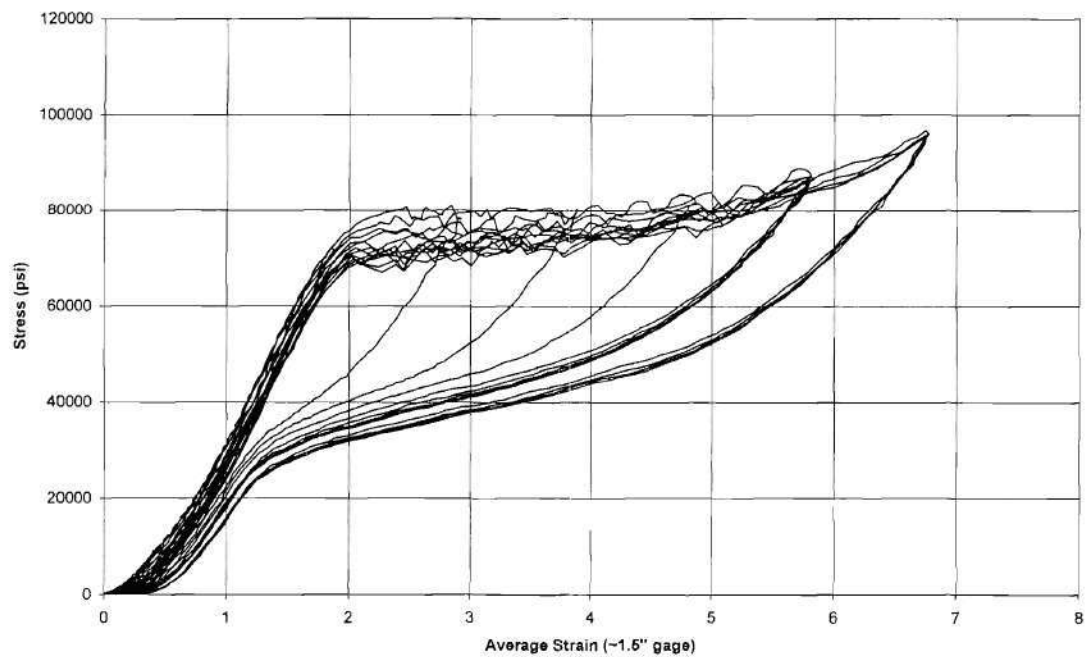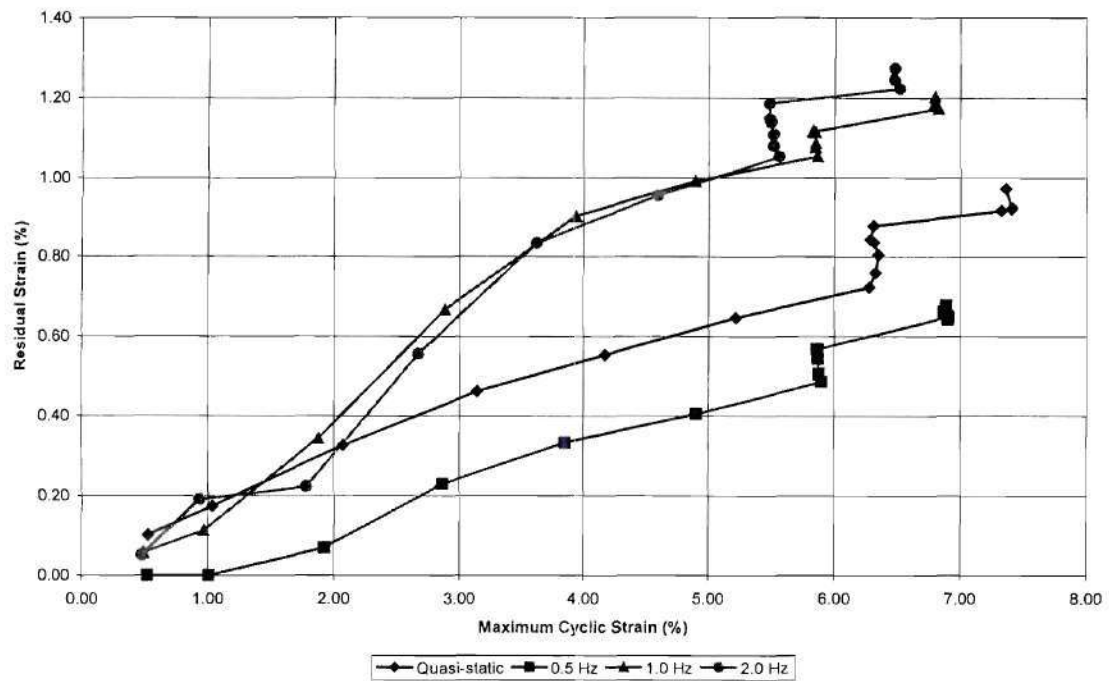
Cyclic Test Results

The plots below show the initial elastic modulus, loading plateau stress, residual strain, and equivalent viscous damping values with respect to the maximum cyclic strain for the 0.01" diameter previously untested NiTi wires tested quasi-statically and dynamically at 0.5 Hz, 1.0 Hz, and 2.0 Hz. The initial elastic modulus plot shows an increase in the austenitic elastic modulus with increased strain rate. The elastic modulus for the specimen tested quasi-statically ranges between approximately 3200 ksi to 3600 ksi where the results for the 0.5 Hz dynamic wire range between approximately 4500 ksi and 4800 ksi. All loading rates show a decrease in elastic modulus with an increase in maximum strain level and increased number of cycles. The loading plateau results show a significant increase in the loading plateau stress with increased strain rate, although there was little difference between the three dynamically tested specimens. The loading plateau stress was measured as the stress at 3% strain for the quasi-static, 0.5 Hz, and 1.0 Hz tests and the stress at 3.5% strain for the 2.0 Hz test based on the stress-strain plots shown earlier. The dynamic effect on the loading plateau stress can be attributed to the thermoelastic nature of the material. The residual strain plots show a measure of the recentering capability of the material and are measured by determining the strain at the zero stress level along the unloading curve. The residual strain increased with the increasing strain levels due to the formation of permanent dislocations. Large strain rates (1.0 Hz and 2.0 Hz) resulted in larger residual strain values, but all specimens had residual strains below 1.4% even when strained up to approximately 7% strain. All specimens maintained good superelastic properties. Finally, the equivalent viscous damping values showed no real strain rate effects except at large strain levels where increased loading rates led to decreases in the equivalent viscous damping values. The maximum equivalent viscous damping was less than 6%.

Initial Elastic Modulus

Loading Plateau Stress

Residual Strain

Equivalent Viscous Damping